

CM Mic and other ER UMa stars showing standstills

Taichi Kato¹, Naoto Kojiguchi¹

¹ Department of Astronomy, Kyoto University, Sakyo-ku, Kyoto 606-8502, Japan
tkato@kusastro.kyoto-u.ac.jp, kojiguchi@kusastro.kyoto-u.ac.jp

Abstract

We analyzed All-Sky Automated Survey for Supernovae (ASAS-SN), Asteroid Terrestrial-impact Last Alert System (ATLAS) and Transiting Exoplanet Survey Satellite (TESS) observations of CM Mic and found that this object belongs to a small group of ER UMa stars showing standstills. In addition to typical ER UMa-type cycles, the object showed standstills between 2017 and 2019 July, and in 2022. The supercycles varied between 49 and 83 d. In 2015, the object showed outbursts with a cycle length of ~ 35 d. An analysis of TESS observations during the 2020 July outburst detected superhumps with a mean period of 0.080251(6) d (value after the full development of superhumps). We also studied other ER UMa stars showing standstills mainly using Zwicky Transient Facility (ZTF) data. DDE 48, MGAB-V728 and ZTF18abmpkbj mostly showed ER UMa-type supercycles but showed one or two standstills. MGAB-V3488 was mostly in ER UMa states with short (~ 25 d) supercycles in 2020–2022 similar to RZ LMi. This object also showed long standstills. PS1-3PI J181732.65+101954.6 showed ER UMa-type supercycles up to 2020 May and entered a long standstill. ZTF18abncpgs showed standstills most of the time, but also showed ER UMa-type supercycles occasionally between standstills. ZTF19aarsljl is a likely member of this group. MGAB-V284 showed a pattern similar to ER UMa stars showing standstills but with a longer time-scale of normal outbursts. This object seems to be an ER UMa star with standstills above the period gap. None of the objects we studied showed a superoutburst arising from a long standstill, as recorded in NY Ser in 2018, although the 2019 June–July superoutburst of PS1-3PI J181732.65+101954.6 might have been an exception.

1 Introduction

ER UMa stars are a small group of SU UMa-type dwarf novae with very short (typically shorter than ~ 80 d)¹ supercycles and frequent normal outbursts (Kato and Kunjaya 1995; Robertson et al. 1995; Patterson et al. 1995; Kato et al. 1999) [normal outbursts, however, can be suppressed, see e.g., Zemko et al. (2013); Ohshima et al. (2014) and normal outbursts sometimes may not occur frequently]. A small number of ER UMa stars and related systems have been recorded to show standstills, which are the defining characteristic of the Z Cam-type dwarf nova [for general information of cataclysmic variables (CVs) and dwarf novae, see e.g., Warner (1995)].

Such objects already reported in the literature are as follows.

- RZ LMi showed long-lasting superoutbursts in 2016–2017 (Kato et al. 2016). The general light curve and the durations of the flat parts are similar to the recently reported standstill of the AM CVn star CR Boo (Kato et al. 2023). It appears that the phenomena recorded in RZ LMi can be interpreted as standstills.
- BK Lyn was originally considered as a novalike object (a CV with a thermally stable disk) (Skillman and Patterson 1993; Ringwald et al. 1996). The object was found to be in an ER UMa state in 2011–2012 (Kemp et al. 2012; Patterson et al. 2013; Kato et al. 2013). The object was probably in this state already in 2005, but not as early as in 2002 (Kato et al. 2013). It returned to the novalike state in 2013 (Kato et al. 2013) and has been in this state since then. This object is probably essentially a novalike object with a transient ER UMa state.
- NY Ser is an SU UMa-type dwarf nova in the period gap (Nogami et al. 1998; Sklyanov et al. 2018). Although supercycles were not as regular as in typical ER UMa stars, the shortest interval of confirmed superoutburst was 97 d (1996 April and July–August, see Nogami et al. 1998). This object also shows long normal outbursts (Pavlenko et al. 2014) and the previous report of a 85 d supercycle [Nogami et al. (1998), adopted in Ritter and Kolb (2003)] is probably an underestimate. Nevertheless, we include this object here as an object related to ER UMa stars. This object showed two standstills and superoutbursts arising from them in 2018 (Kato et al. 2019). This was the first demonstration that the disk radius can increase during standstills.

¹Short supercycles are a result of high mass-transfer rates. As Osaki (1995) showed, however, supercycles can become longer when superoutbursts are long and their durations comprise most of a supercycle, as we will see in RZ LMi and CM Mic in 2020. This situation should be distinguished from systems with long supercycles but with short superoutbursts (i.e. ordinary SU UMa stars).

- MGAB-V859 and ZTF18abgjsdg were reported in Kato and Kojiguchi (2021) showing standstill phases in addition to ER UMa-type behavior.
- WFI J161953.3+031909 is an eclipsing object showing both a standstill and ER UMa states (Kato 2022b).

ER UMa stars are considered to have higher mass-transfer rates than expected from the standard evolutionary sequence of CVs, and are suspected to be descendants of old novae (see e.g., Patterson et al. 2013). The presence of standstills also favors a high mass-transfer rate as required by the disk instability theory (see e.g., Osaki 1996).

ER UMa stars showing standstills have additional implications: they are probably a result of variable mass-transfer rates and how such standstills evolve provides a clue in understanding the evolution of the disk radius or the angular momentum in the accretion disk (Kato et al. 2019), which is still an unsolved problem (e.g., Kimura et al. 2020).

In this paper, we show that CM Mic (=EC 20335–4332) is yet another member of this small group of CVs. This object was initially selected as a DC white dwarf (CS 22943-206; Beers et al. 1992). Chen et al. (2001) classified it as a possible dwarf nova with a range of $B=14.9\text{--}15.9$. Kazarovets et al. (2003) gave a variable star name CM Mic and classified it as a novalike. This object did not receive much attention and it was only 2018 when the object was classified as a Z Cam star based on the All-Sky Automated Survey for Supernovae (ASAS-SN, Shappee et al. 2014, Kochanek et al. 2017) observations (T. Kato, vsnet-chat 8095²). Using ASAS-SN and Transiting Exoplanet Survey Satellite (TESS) observations (Ricker et al. 2015)³, this object was also identified as an ER UMa star (N. Kojiguchi, vsnet-chat 8992⁴).

2 Data analysis

We used ASAS-SN observations and Asteroid Terrestrial-impact Last Alert System (ATLAS; Tonry et al. 2018) forced photometry (Shingles et al. 2021) to examine the long-term behavior.

We used TESS observations, which recorded the initial part of the 2020 July superoutburst, to analyze superhumps. Superhumps maxima were determined using the template fitting method introduced in Kato et al. (2009) after removing outburst trends by locally-weighted polynomial regression (LOWESS; Cleveland 1979). The periods were determined using the phase dispersion minimization (PDM; Stellingwerf 1978) method, whose errors were estimated by the methods of Fernie (1989); Kato et al. (2010). We also used Zwicky Transient Facility (ZTF; Masci et al. 2019)⁵ data for analysis of other objects given in section 4.

3 Results

3.1 Long-term behavior

Long-term light curves based on ASAS-SN and ATLAS data are shown in figures 1 and 2.

In figure 1, the object showed outbursts with a cycle length of ~ 35 d in 2015 (second panel). This pattern became weaker in 2016 (third panel). The object stayed in standstill in 2017 and 2018 (fourth and fifth panels). The behavior in 2014 (first panel) was likely similar to 2015, but was uncertain due to the limited quality of the ASAS-SN data.

In figure 2, the object was initially in standstill (first panel) with some hint of low-amplitude oscillation with a period of 20–30 d. The object entered a dwarf nova state after BJD 2458680 (2019 July 15), followed by a superoutburst on BJD 2458714 (2019 August 18)⁶. This superoutburst lasted long (~ 55 d), as in long superoutbursts or superoutbursts with a standstill in RZ LMi (Kato et al. 2016). The supercycle was 83 d. In 2020 (second panel), the object showed shorter supercycles (49–70 d) with some structures in the fading part of the superhumps (such as at BJD 2459000 and 2459068). In 2021 (third panel), the object showed a more typical

²<http://ooruri.kusastro.kyoto-u.ac.jp/mailarchive/vsnet-chat/8095>.

³<https://tess.mit.edu/observations/>. The full light-curve is available at the Mikulski Archive for Space Telescope (MAST, <http://archive.stsci.edu/>).

⁴<http://ooruri.kusastro.kyoto-u.ac.jp/mailarchive/vsnet-chat/8992>.

⁵The ZTF data can be obtained from IRSA <https://irsa.ipac.caltech.edu/Missions/ztf.html> using the interface https://irsa.ipac.caltech.edu/docs/program_interface/ztf_api.html or using a wrapper of the above IRSA API <https://github.com/MickaelRigault/ztfquery>.

⁶We assume that all long outbursts in this object are superoutbursts based on the detection of superhumps during one of long outbursts in the TESS data (subsection 3.2).

ER UMa-type variation with many normal outbursts but with variable supercycles (53–67 d) and variable shapes of superoutbursts. The superoutburst starting on BJD 2459465 (2021 September 7) showed brightening in the later part (BJD 2459488, 2021 October 1) as in 2020. The object was in standstill again in 2022 (fourth panel). It has been in an ER UMa state in 2023 again (fifth panel). The ER UMa-type behavior in 2020 and 2021 is shown in more detail in an expanded scale in figures 3 and 4.

3.2 TESS observations

The times of superhump maxima are listed in table 1. The $O - C$ variation together with the variation of superhump amplitudes and the light curve is shown in figure 5. The peak of the superhump amplitudes occurred around $E=19$. TESS observations covered superhump stages A and B [see Kato et al. (2009); Kato (2022c) for superhump stages]. Using the linear part $2 \leq E \leq 12$, we obtained a period of 0.0817(2) d for stage A superhumps. It was somewhat ambiguous to define when stage B started. Using the range $30 \leq E \leq 262$, the mean superhump period (P_{SH}) was 0.080251(6) d and the period derivative ($P_{\text{dot}} = \dot{P}/P$) was $+2.0(2) \times 10^{-5}$. Using the range $50 \leq E \leq 262$, these values were $P_{\text{SH}} = 0.080253(8)$ d and $P_{\text{dot}} = +2.9(3) \times 10^{-5}$. The small positive P_{dot} was similar to $+4(2) \times 10^{-5}$ for ER UMa (Kato et al. 2009) and $+3(3) \times 10^{-5}$ for BK Lyn (Kato et al. 2013). As shown in Kato and Osaki (2013); Kato (2022a), the mass ratio can be determined from the stage A superhump period if the orbital period is known. In the case of CM Mic, the orbital signal was not detected in the available TESS data and this is a future task possibly requiring a radial-velocity study. A PDM analysis and the mean profile of superhumps from TESS observations are shown in figure 6. The mean period (entire data with stages A and B combined) was 0.080276(5) d.

The variation of the superhump profile is shown in figures 7, 8 and 9. Figure 7 contains stage A and the early phase of stage B. The amplitudes of the superhumps grew quickly and the period became shorter (early stage B). Figures 8 and 9 show the evolution in stage B. The superhump amplitudes decayed with lengthening of the superhump period, as shown in the $O - C$ analysis. No phase reversal was observed as in ER UMa (Kato et al. 1996, 2003). This result suggests diversity in evolution of superhumps among ER UMa stars.

This superoutburst showed brightening in the later phase (subsection 3.1). In ordinary SU UMa stars, stage C superhumps and an increase in the superhump amplitude are usually associated with such brightening (see e.g., Kato et al. 2009; Kato 2022c). It was unclear whether the same thing happened in CM Mic due to the lack of time-resolved photometric data.

4 Long-term light curves of other ER UMa stars with standstills

4.1 DDE 48

DDE 48 is a dwarf nova discovered by D. Denisenko in 2016 (vsnet-alert 20146⁷). This object was identified as an ER UMa star based on the detection of superhumps with a period of 0.067 d and frequent normal outbursts (D. Denisenko, vsnet-alert 20291⁸). A superhump was also reported in Kato et al. (2017). TESS observations in 2022 August also recorded a superoutburst (N. Kojiguchi in prep.). The object was also classified as a Z Cam star by the detection of a standstill in ZTF data (T. Kato, vsnet-chat 9059⁹).

The long-term light curve is shown in figures 10 and 11. The object showed ER UMa-type supercycles most of the time. There was a standstill between BJD 2458826 (2019 December 8) and BJD 2458993 (2020 May 23). The two superoutbursts preceding this standstill had longer durations than the typical ones in this system (first panel of figure 10) and there was a shallow dip amid the superoutburst plateau (BJD 2458770–2458777) just like in some superoutbursts in CM Mic. The lengthening of superoutbursts toward the standstill was probably a manifestation of the increasing mass-transfer rate. Just before the end of the standstill, small-amplitude oscillations appeared. This probably reflected a part of the disk becoming thermally unstable due to the decreasing mass-transfer rate. This object is also known as PS1-3PI J204611.81+242057.2 (Sesar et al. 2017), ATO J311.5492+24.3492 (Heinze et al. 2018) and a Gaia variable Gaia DR3 1843254106354614272 (type CV) (Gaia Collaboration et al. 2022).

⁷<<http://ooruri.kusastro.kyoto-u.ac.jp/mailarchive/vsnet-alert/20146>>.

⁸<<http://ooruri.kusastro.kyoto-u.ac.jp/mailarchive/vsnet-alert/20291>>.

⁹<<http://ooruri.kusastro.kyoto-u.ac.jp/mailarchive/vsnet-chat/9059>>.

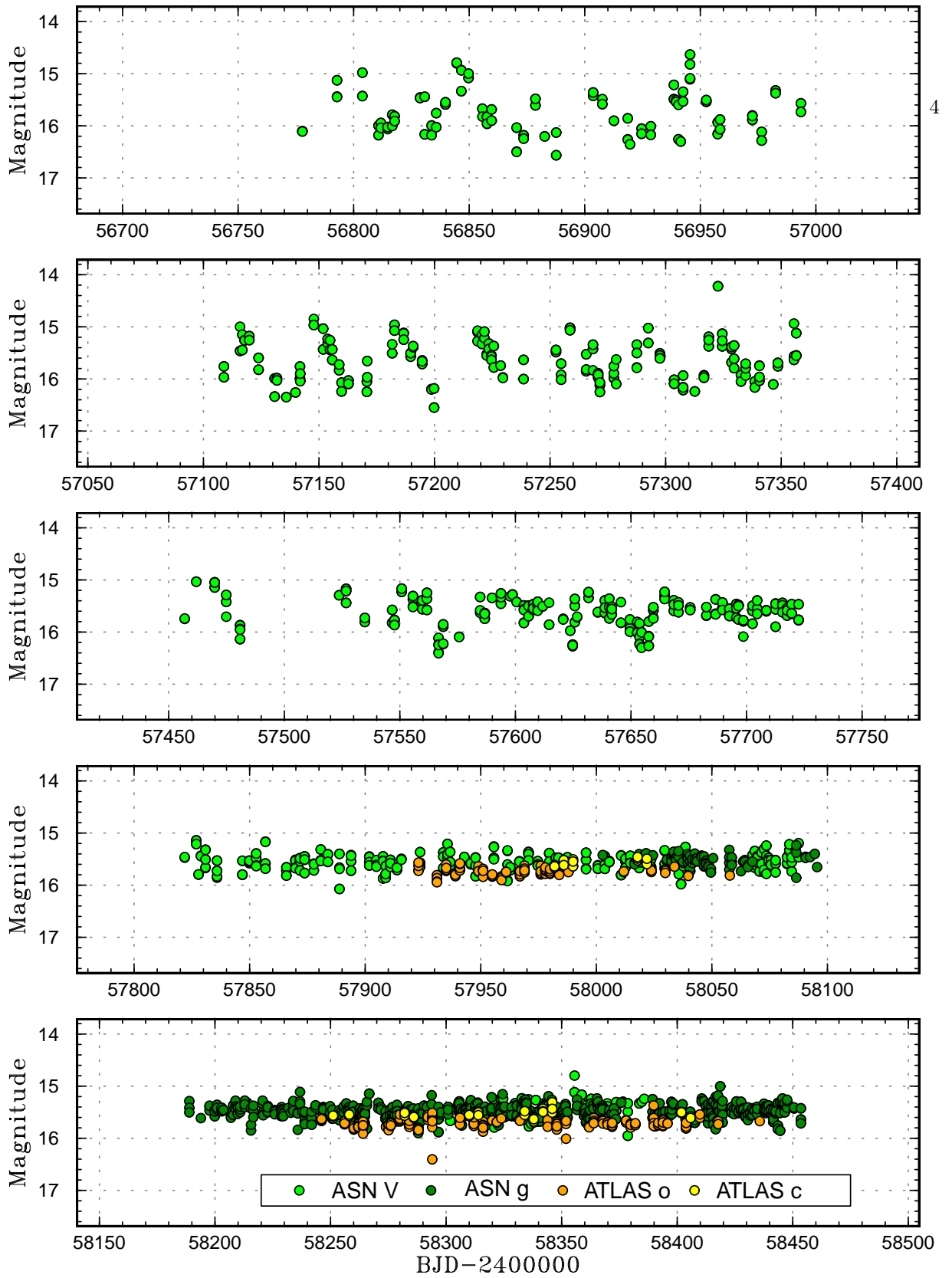


Figure 1: Light curve of CM Mic in 2014–2018. The object showed outbursts with a cycle length of ~ 35 d in 2015 (second panel). This pattern became weaker in 2016 (third panel). The object stayed in standstill in 2017 and 2018 (fourth and fifth panels). ASN refer to ASAS-SN observations.

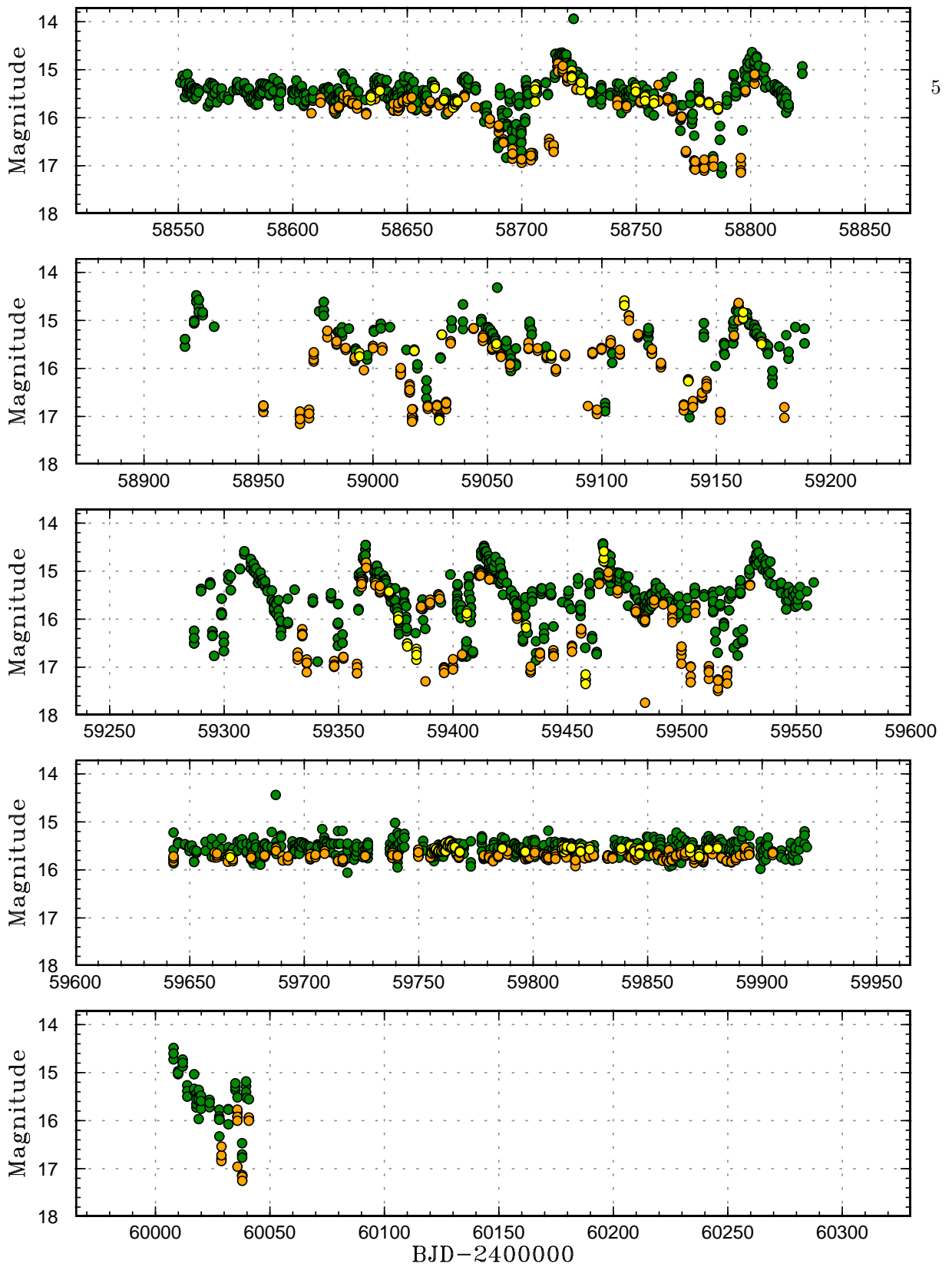


Figure 2: Light curve of CM Mic in 2019–2023. The symbols are the same as in figure 1.

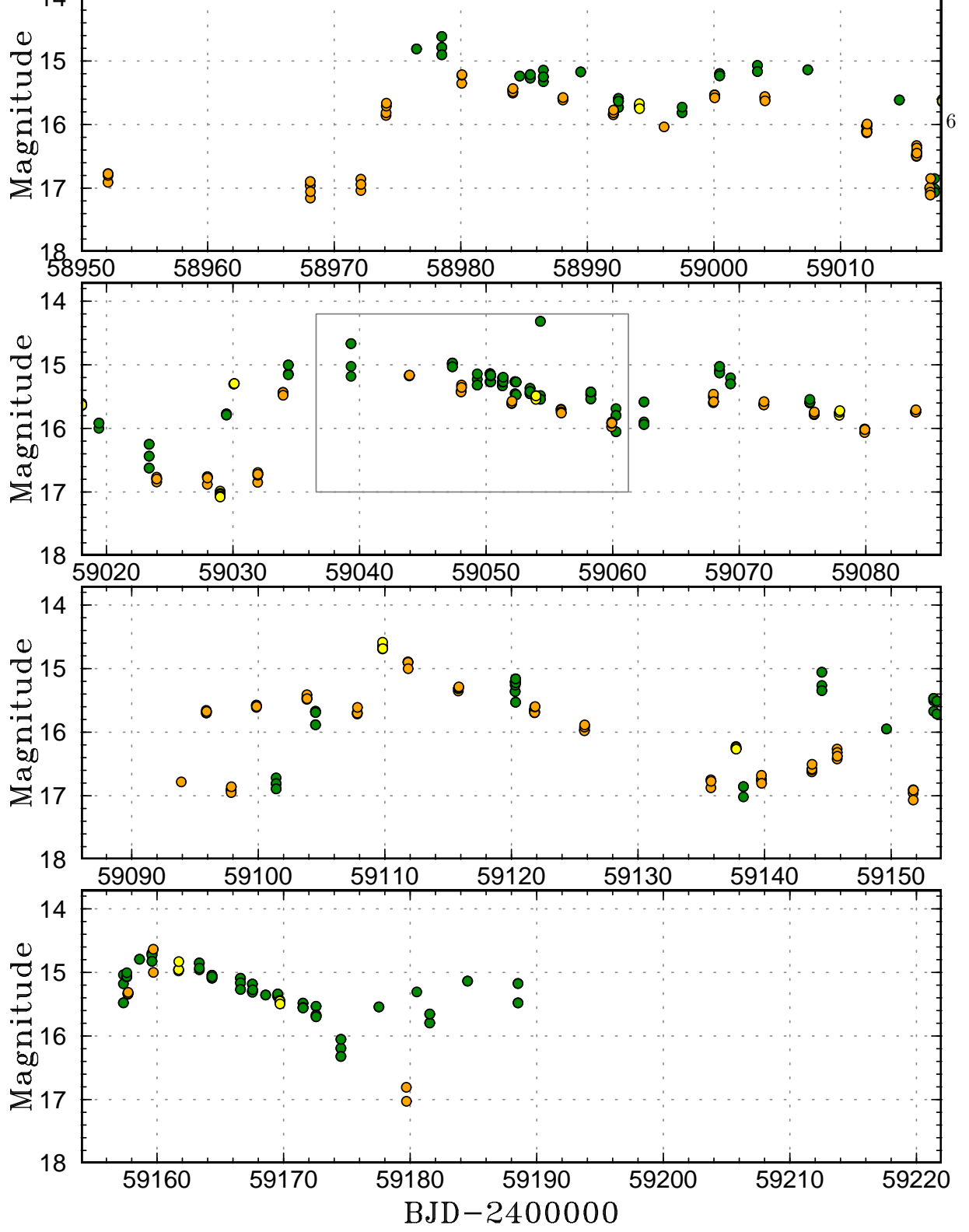


Figure 3: ER Uma state of CM Mic in 2020. The symbols are the same as in figure 1. The first and second superoutbursts (first and second panels, respectively) were long and were associated with brightening in the later phase. The grey box indicates the range of figure 5.

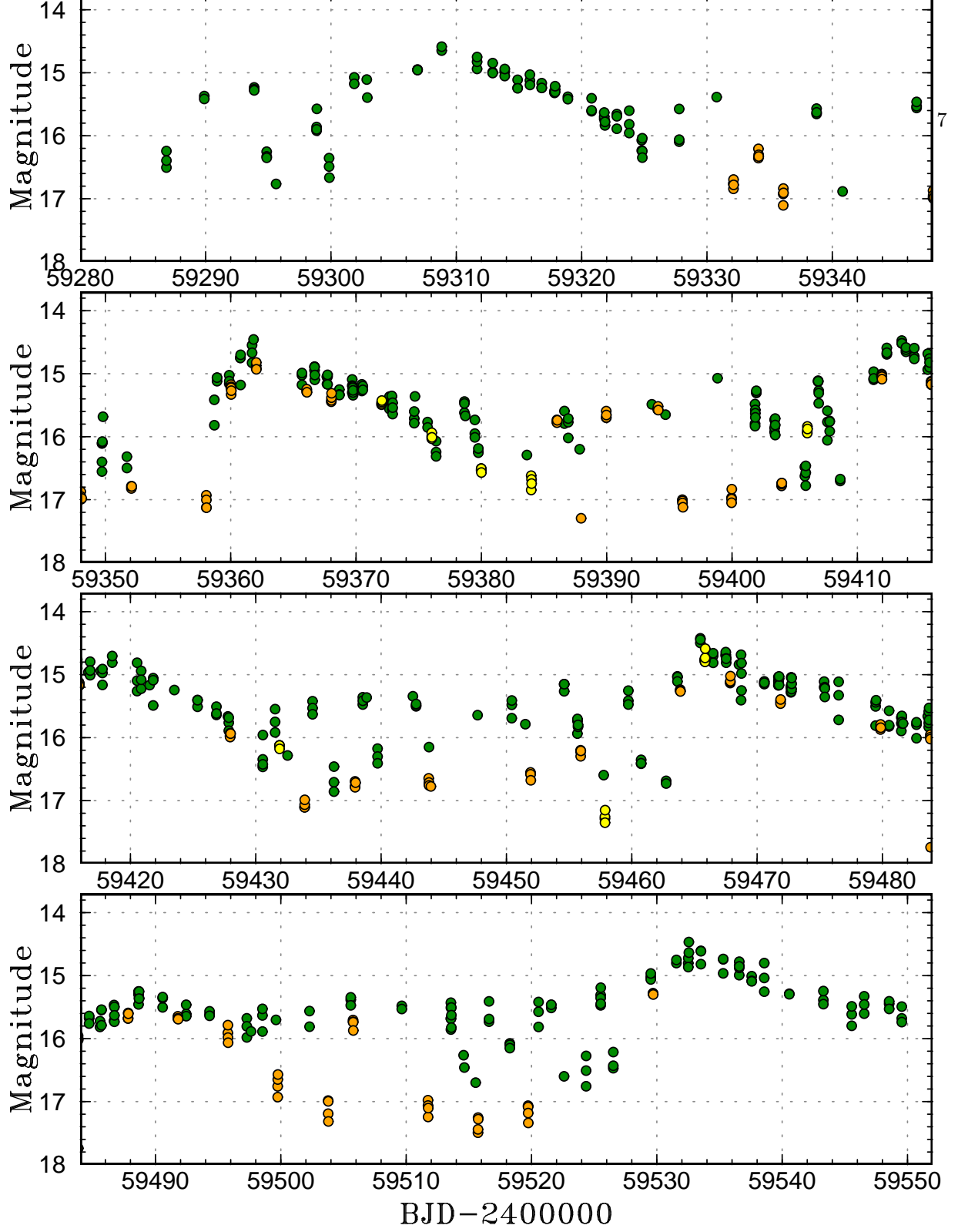


Figure 4: ER Uma state of CM Mic in 2021. The symbols are the same as in figure 1. Supercycles became shorter and more regular than in 2020.

Table 1: Times of superhump maxima in CM Mic

E	T^*	error	amp [†]	E	T	error	amp	E	T	error	amp
0	39.4563	0.0049	0.028	47	43.2410	0.0013	0.125	94	47.0159	0.0016	0.156
1	39.5368	0.0025	0.054	48	43.3173	0.0016	0.119	95	47.0941	0.0017	0.113
2	39.6121	0.0024	0.066	49	43.4004	0.0017	0.094	96	47.1758	0.0017	0.112
3	39.6893	0.0011	0.109	50	43.4777	0.0009	0.126	97	47.2535	0.0024	0.072
4	39.7751	0.0013	0.114	51	43.5613	0.0021	0.092	98	47.3364	0.0014	0.149
5	39.8528	0.0008	0.126	52	43.6409	0.0017	0.109	99	47.4118	0.0021	0.073
6	39.9393	0.0008	0.137	53	43.7211	0.0012	0.123	100	47.4942	0.0020	0.107
7	40.0200	0.0007	0.164	54	43.7982	0.0028	0.058	101	47.5730	0.0021	0.097
8	40.1033	0.0011	0.114	55	43.8848	0.0018	0.080	102	47.6570	0.0022	0.081
9	40.1811	0.0011	0.148	56	43.9687	0.0020	0.077	103	47.7386	0.0034	0.058
10	40.2647	0.0009	0.161	57	44.0455	0.0016	0.109	104	47.8141	0.0019	0.098
11	40.3460	0.0008	0.165	58	44.1257	0.0018	0.088	105	47.8918	0.0019	0.116
12	40.4270	0.0009	0.169	59	44.2008	0.0016	0.105	106	47.9736	0.0032	0.066
13	40.5068	0.0007	0.201	60	44.2797	0.0024	0.089	107	48.0563	0.0018	0.093
14	40.5892	0.0007	0.179	61	44.3703	0.0026	0.055	108	48.1337	0.0092	0.047
15	40.6676	0.0007	0.217	62	44.4480	0.0016	0.111	121	49.1790	0.0024	0.083
16	40.7498	0.0006	0.239	63	44.5288	0.0020	0.103	122	49.2571	0.0019	0.091
17	40.8301	0.0006	0.198	64	44.6079	0.0021	0.090	123	49.3343	0.0023	0.065
18	40.9117	0.0005	0.240	65	44.6858	0.0027	0.080	124	49.4166	0.0017	0.094
19	40.9909	0.0005	0.219	66	44.7666	0.0014	0.154	125	49.4982	0.0021	0.071
20	41.0711	0.0006	0.245	67	44.8463	0.0025	0.078	126	49.5800	0.0077	0.023
21	41.1507	0.0006	0.219	68	44.9268	0.0018	0.111	127	49.6541	0.0022	0.063
22	41.2314	0.0006	0.214	69	45.0084	0.0026	0.074	128	49.7341	0.0021	0.071
23	41.3121	0.0007	0.205	70	45.0875	0.0017	0.131	129	49.8176	0.0027	0.063
24	41.3932	0.0006	0.197	71	45.1647	0.0026	0.097	130	49.8945	0.0024	0.085
25	41.4751	0.0009	0.168	72	45.2481	0.0027	0.075	131	49.9800	0.0033	0.050
26	41.5539	0.0007	0.209	73	45.3306	0.0015	0.136	132	50.0578	0.0047	0.044
27	41.6330	0.0009	0.161	74	45.4105	0.0022	0.089	133	50.1409	0.0018	0.090
28	41.7151	0.0007	0.161	75	45.4922	0.0030	0.062	134	50.2201	0.0018	0.070
29	41.7974	0.0009	0.181	76	45.5689	0.0019	0.108	135	50.3042	0.0019	0.077
30	41.8756	0.0008	0.146	77	45.6506	0.0020	0.096	136	50.3783	0.0018	0.086
31	41.9559	0.0008	0.167	78	45.7268	0.0055	0.045	137	50.4581	0.0019	0.079
32	42.0388	0.0009	0.164	79	45.8132	0.0024	0.080	138	50.5389	0.0014	0.100
33	42.1166	0.0008	0.159	80	45.8916	0.0017	0.098	139	50.6250	0.0045	0.041
34	42.1977	0.0009	0.157	81	45.9728	0.0018	0.108	140	50.6971	0.0022	0.098
35	42.2769	0.0011	0.153	82	46.0506	0.0030	0.063	141	50.7843	0.0022	0.075
36	42.3588	0.0011	0.123	83	46.1302	0.0020	0.094	142	50.8654	0.0050	0.034
37	42.4404	0.0011	0.132	84	46.2147	0.0019	0.097	143	50.9418	0.0025	0.080
38	42.5179	0.0012	0.138	85	46.2933	0.0020	0.104	144	51.0212	0.0022	0.081
39	42.6001	0.0014	0.112	86	46.3733	0.0018	0.080	145	51.0972	0.0020	0.096
40	42.6790	0.0010	0.173	87	46.4543	0.0019	0.096	146	51.1821	0.0026	0.074
41	42.7605	0.0012	0.157	88	46.5343	0.0019	0.111	147	51.2605	0.0029	0.064
42	42.8385	0.0012	0.167	89	46.6157	0.0032	0.062	148	51.3414	0.0020	0.092
43	42.9202	0.0017	0.076	90	46.6961	0.0017	0.104	149	51.4195	0.0015	0.093
44	42.9978	0.0015	0.116	91	46.7743	0.0013	0.146	150	51.5047	0.0029	0.056
45	43.0806	0.0012	0.150	92	46.8549	0.0015	0.142	151	51.5828	0.0029	0.068
46	43.1586	0.0014	0.127	93	46.9355	0.0024	0.071	152	51.6621	0.0014	0.114

*BJD-2459000.

†Amplitude (mag).

Table 1: Times of superhump maxima in CM Mic (continued)

E	T^*	error	amp [†]	E	T	error	amp	E	T	error	amp
153	51.7468	0.0033	0.059	186	1054.3936	0.0062	0.032	215	56.7218	0.0041	0.076
154	51.8280	0.0035	0.051	187	1054.4696	0.0022	0.082	216	56.8002	0.0040	0.069
155	51.9016	0.0026	0.080	188	1054.5481	0.0046	0.049	217	56.8850	0.0066	0.068
156	51.9807	0.0028	0.062	189	1054.6308	0.0048	0.051	219	57.0423	0.0042	0.049
157	52.0595	0.0051	0.052	190	1054.7045	0.0034	0.069	220	57.1224	0.0030	0.058
158	52.1424	0.0026	0.089	191	1054.7962	0.0087	0.026	221	57.2112	0.0039	0.094
159	52.2193	0.0023	0.087	192	1054.8770	0.0027	0.083	223	57.3716	0.0045	0.059
160	52.3036	0.0025	0.061	193	1054.9523	0.0035	0.071	225	57.5244	0.0036	0.066
161	52.3827	0.0046	0.039	194	1055.0409	0.0016	0.128	226	57.6030	0.0035	0.078
162	52.4602	0.0031	0.056	195	1055.1157	0.0042	0.055	228	57.7660	0.0035	0.086
163	52.5435	0.0022	0.080	196	1055.1927	0.0056	0.042	229	57.8520	0.0044	0.077
165	52.7023	0.0030	0.064	197	1055.2714	0.0046	0.054	231	58.0152	0.0036	0.056
166	52.7873	0.0037	0.053	198	1055.3530	0.0026	0.068	233	58.1705	0.0046	0.075
168	52.9489	0.0037	0.046	199	1055.4296	0.0025	0.087	234	58.2540	0.0029	0.060
169	53.0260	0.0020	0.088	201	1055.5918	0.0038	0.067	236	58.4187	0.0035	0.098
170	53.0997	0.0020	0.110	202	1055.6712	0.0042	0.056	237	58.4988	0.0044	0.087
171	53.1865	0.0028	0.081	203	1055.7518	0.0030	0.088	241	58.8211	0.0059	0.073
172	53.2646	0.0053	0.038	204	1055.8354	0.0059	0.036	241	58.8204	0.0121	0.047
173	53.3451	0.0030	0.061	206	1055.9929	0.0042	0.058	244	59.0727	0.0076	0.023
174	53.4288	0.0046	0.039	207	1056.0772	0.0058	0.039	245	59.1326	0.0052	0.044
175	53.5043	0.0028	0.060	208	1056.1701	0.0074	0.031	247	59.2857	0.0054	0.052
176	53.5821	0.0026	0.081	209	1056.2422	0.0044	0.054	249	59.4644	0.0030	0.051
177	53.6605	0.0033	0.057	210	1056.3070	0.0055	0.050	250	59.5375	0.0079	0.078
178	53.7430	0.0037	0.052	211	1056.4045	0.0016	0.130	258	60.1970	0.0033	0.045
181	53.9939	0.0035	0.062	212	1056.4779	0.0037	0.061	259	60.2547	0.0054	0.095
183	54.1415	0.0028	0.070	213	1056.5604	0.0019	0.102	261	60.4252	0.0042	0.058
184	54.2243	0.0031	0.061	214	1056.6408	0.0034	0.076	262	60.5107	0.0045	0.072

*BJD-2459000.

†Amplitude (mag).

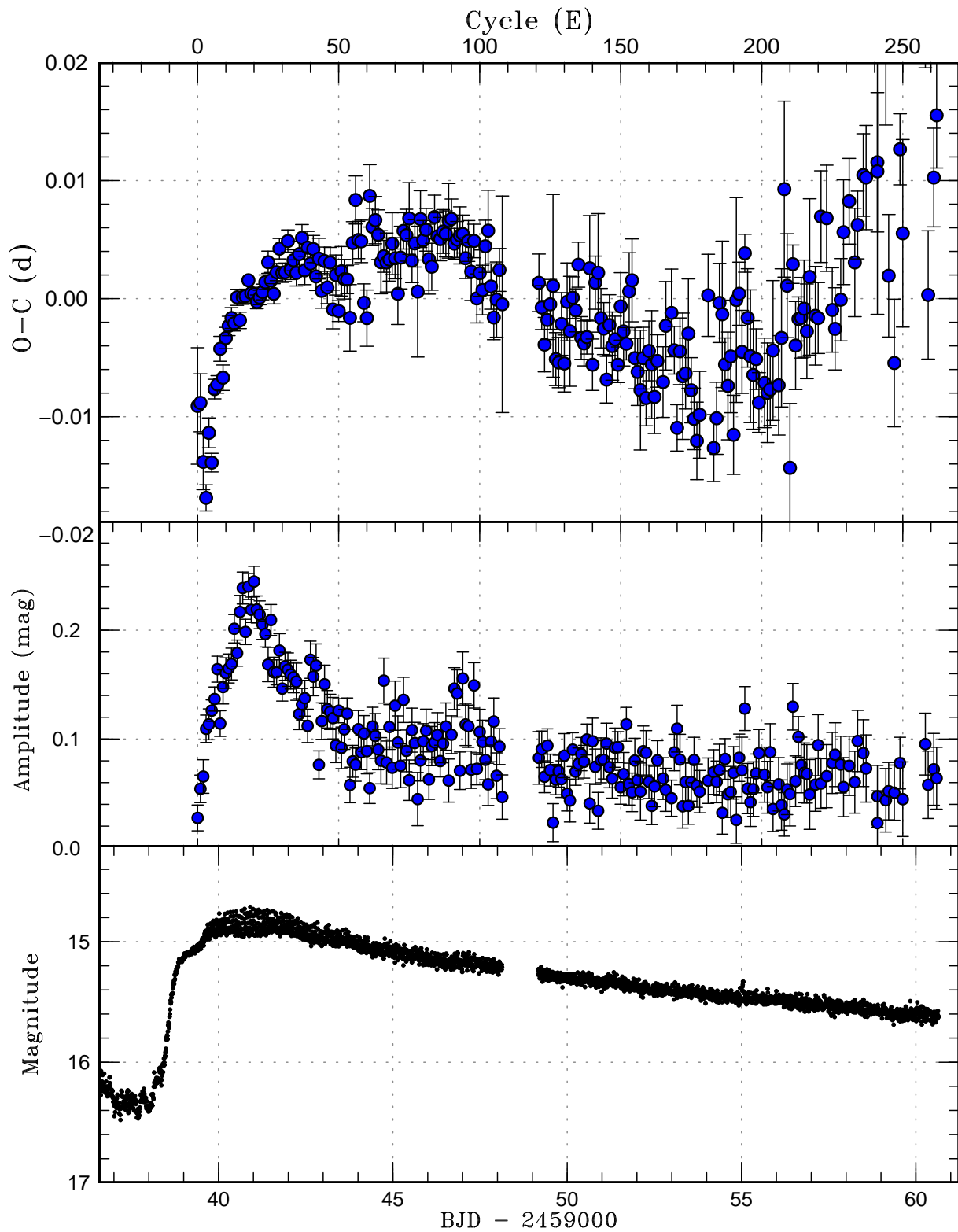


Figure 5: TESS observations of superhumps of CM Mic during the 2020 July superoutburst. (Upper:) $O - C$ variation. The ephemeris of $\text{BJD}(\text{max}) = 2459039.4000 + 0.08090E$ was used. The data are in table 1. (Middle:) Superhump amplitude. (Lower:) TESS light curve. The data were binned to 0.008 d.

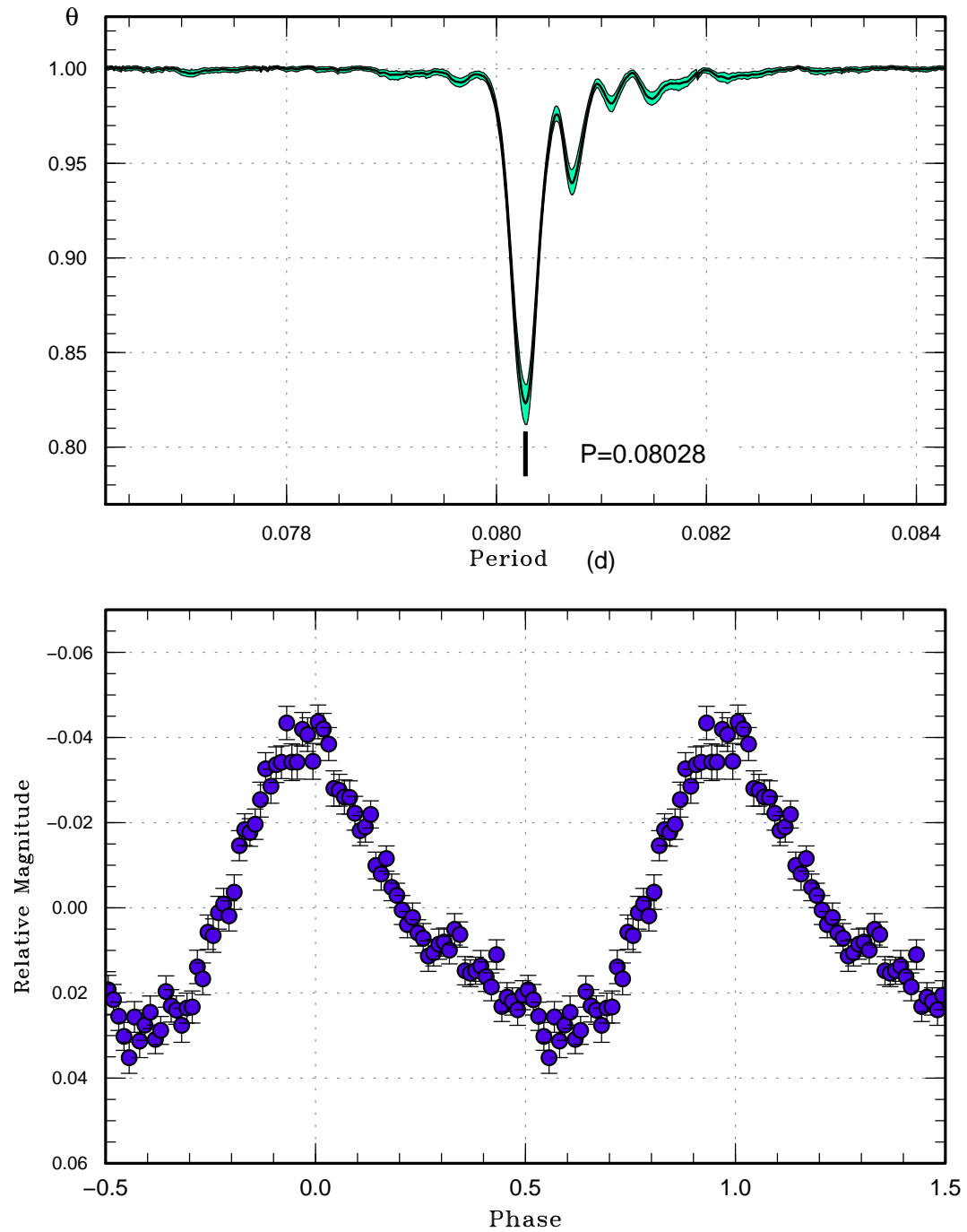


Figure 6: Mean superhump profile of CM Mic from TESS data (range after BJD 2459039.4). (Upper): PDM analysis. The bootstrap result using randomly contain 50% of observations is shown as a form of 90% confidence intervals in the resultant θ statistics. (Lower): Phase plot.

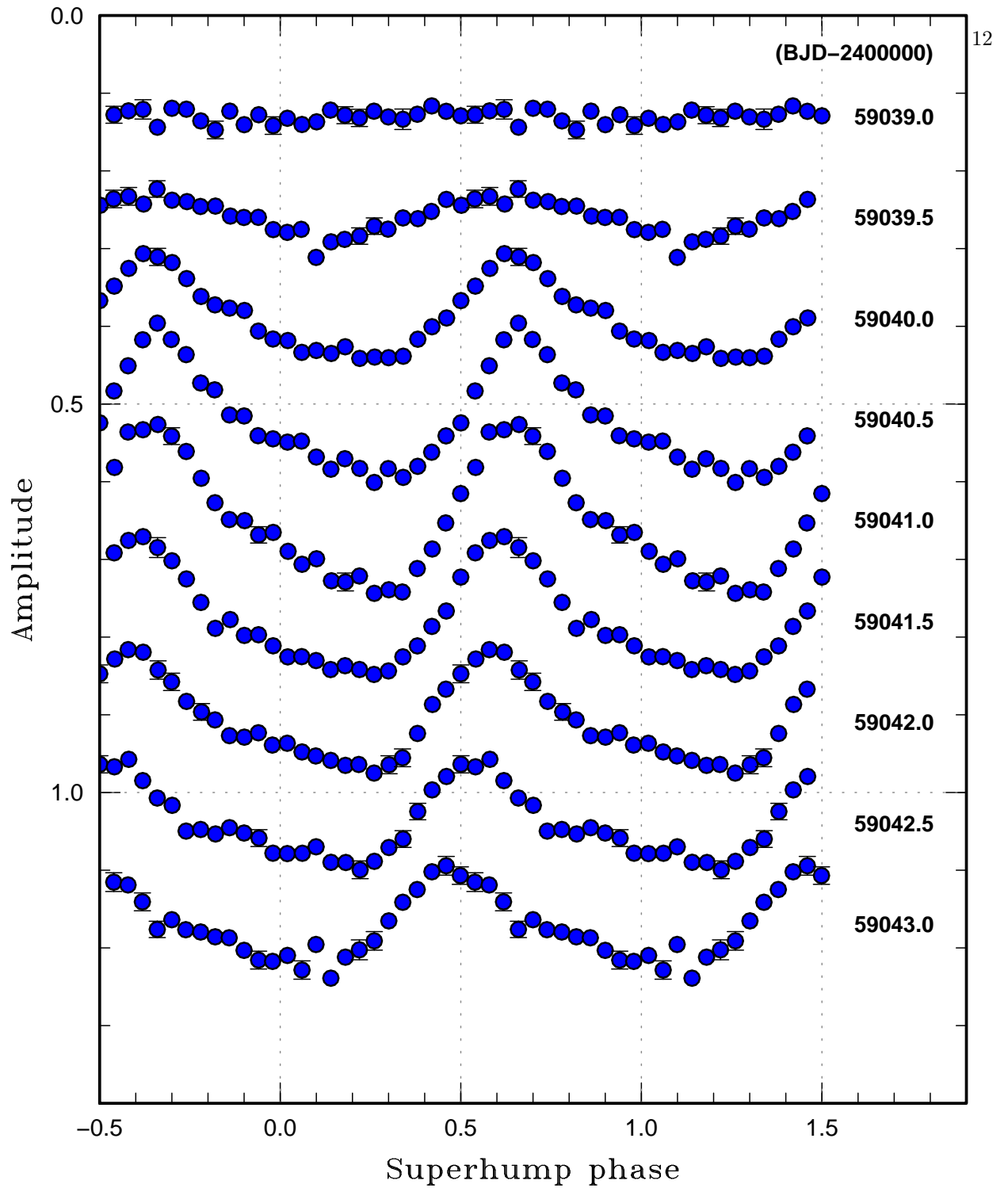


Figure 7: Variation of profiles of superhumps in the growing phase (stage A) to the initial part of stage B. The zero phase and superhump period were defined as BJD 2459039.4000 and 0.08090 d (same as in figure 5). 0.5-d segments were used whose centers are shown on the right side of the figure. The superhump period was long up to BJD 2459040.5 and then became short.

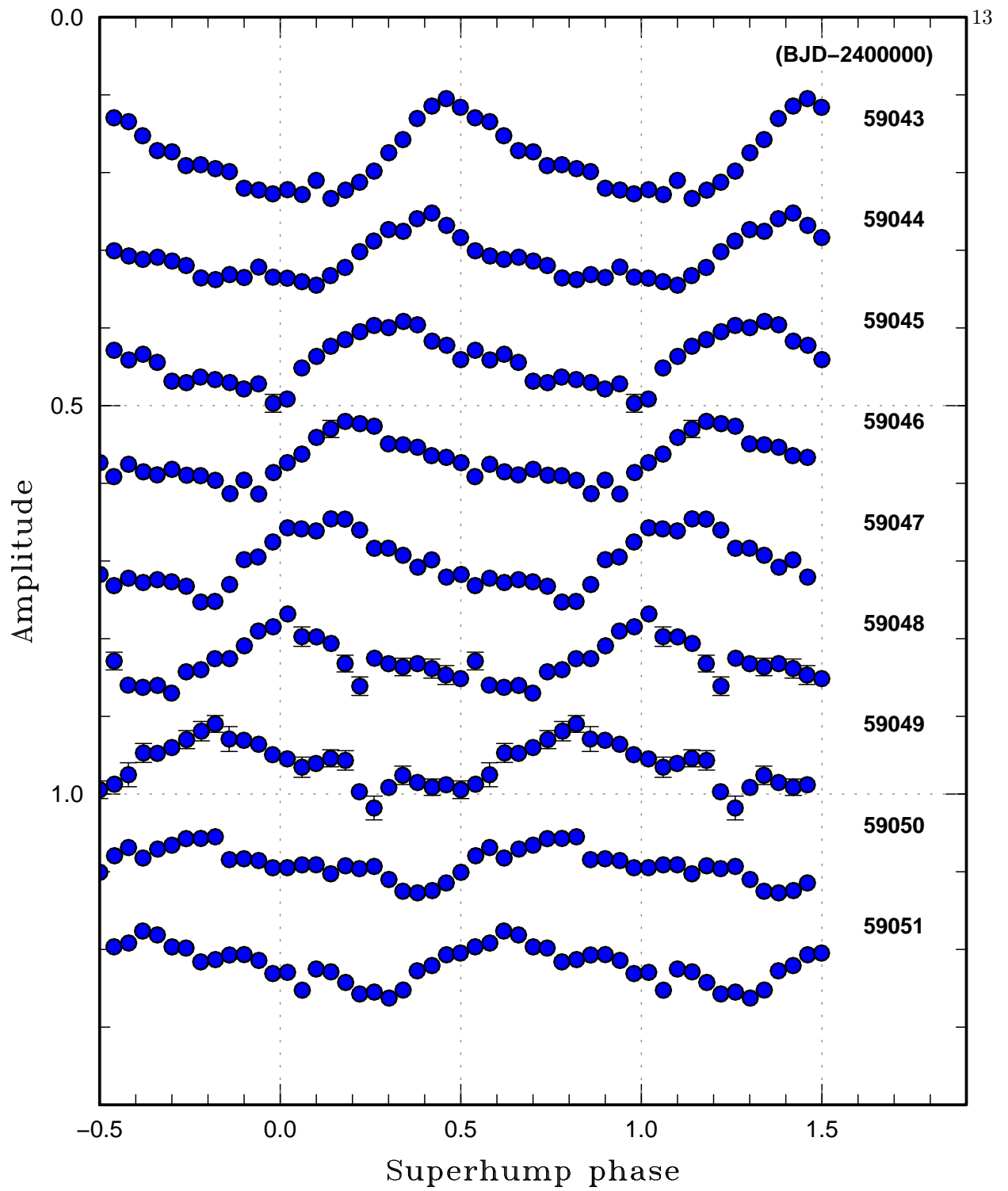


Figure 8: Variation of profiles of superhumps in the early part of stage B. 1-d segments were used whose centers are shown on the right side of the figure. The zero phase and superhump period were the same as in figure 7.

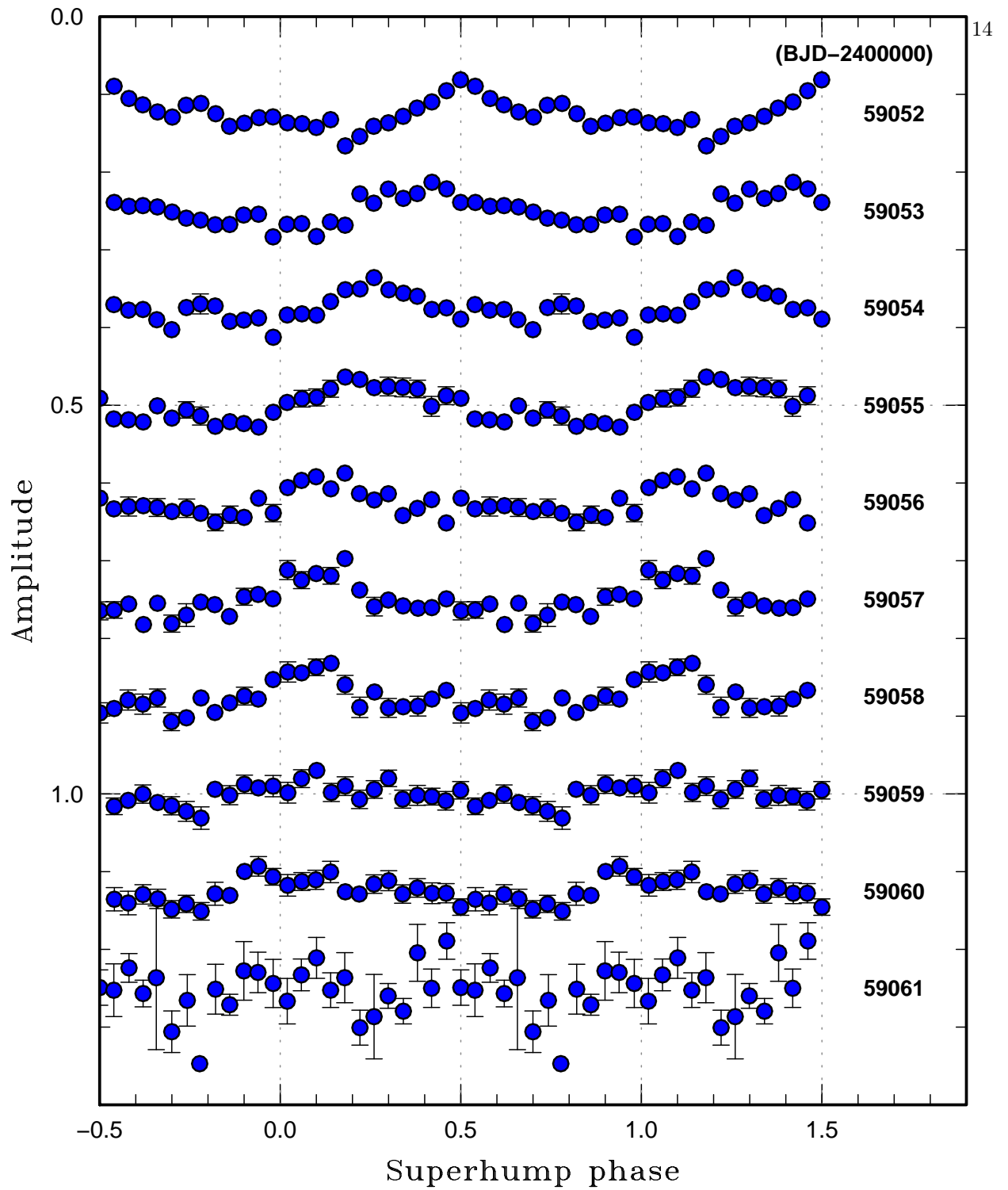


Figure 9: Variation of profiles of superhumps in the late part of stage B. 1-d segments were used whose centers are shown on the right side of the figure. The zero phase and superhump period were the same as in figure 7. Superhumps decayed and the period became longer than in figure 8.

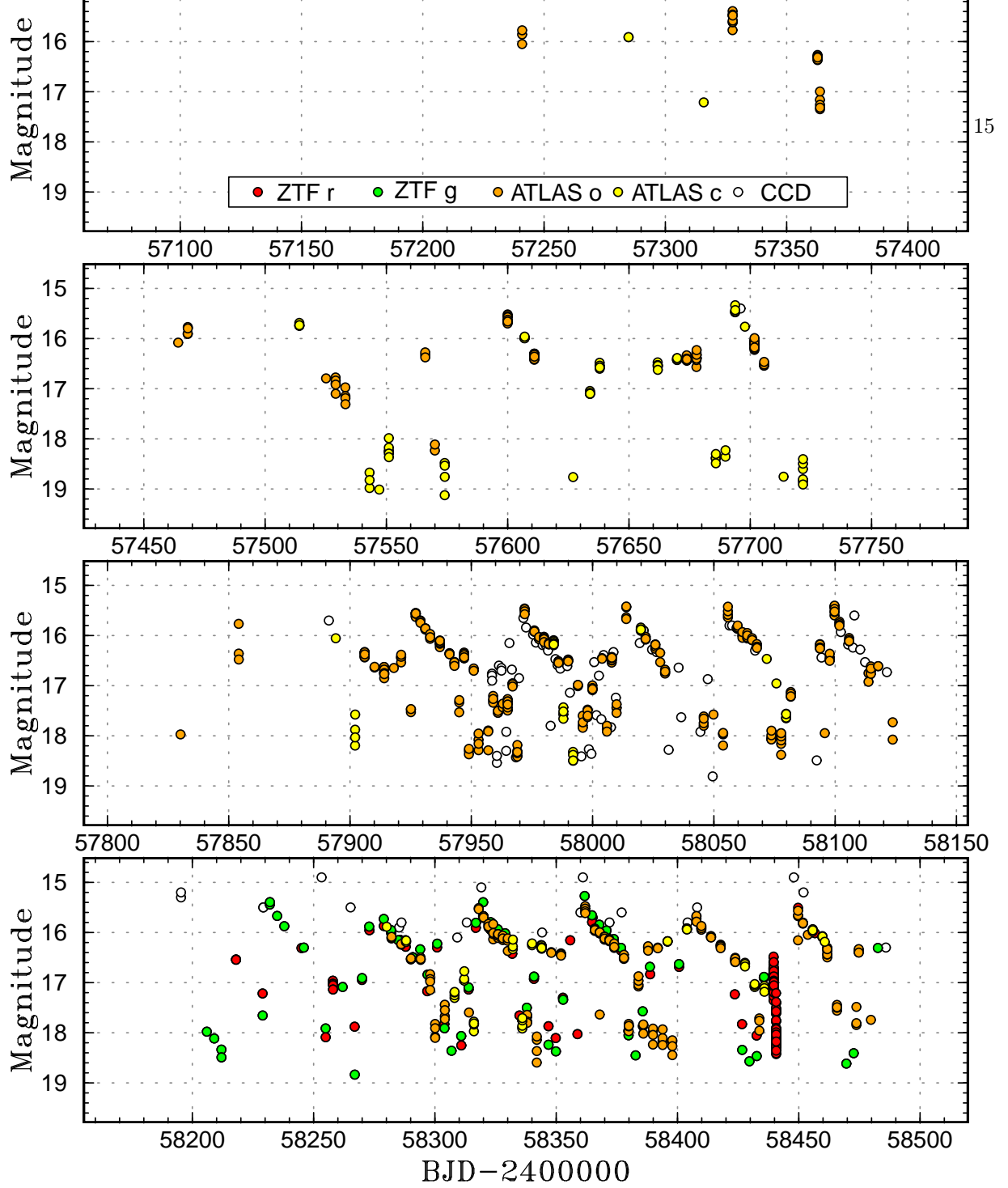


Figure 10: Light curve of DDE 48 in 2015–2018. The object mostly showed ER UMa-type supercycles. CCD refer to snapshot unfiltered CCD observations reported to VSOLJ and VSNET.

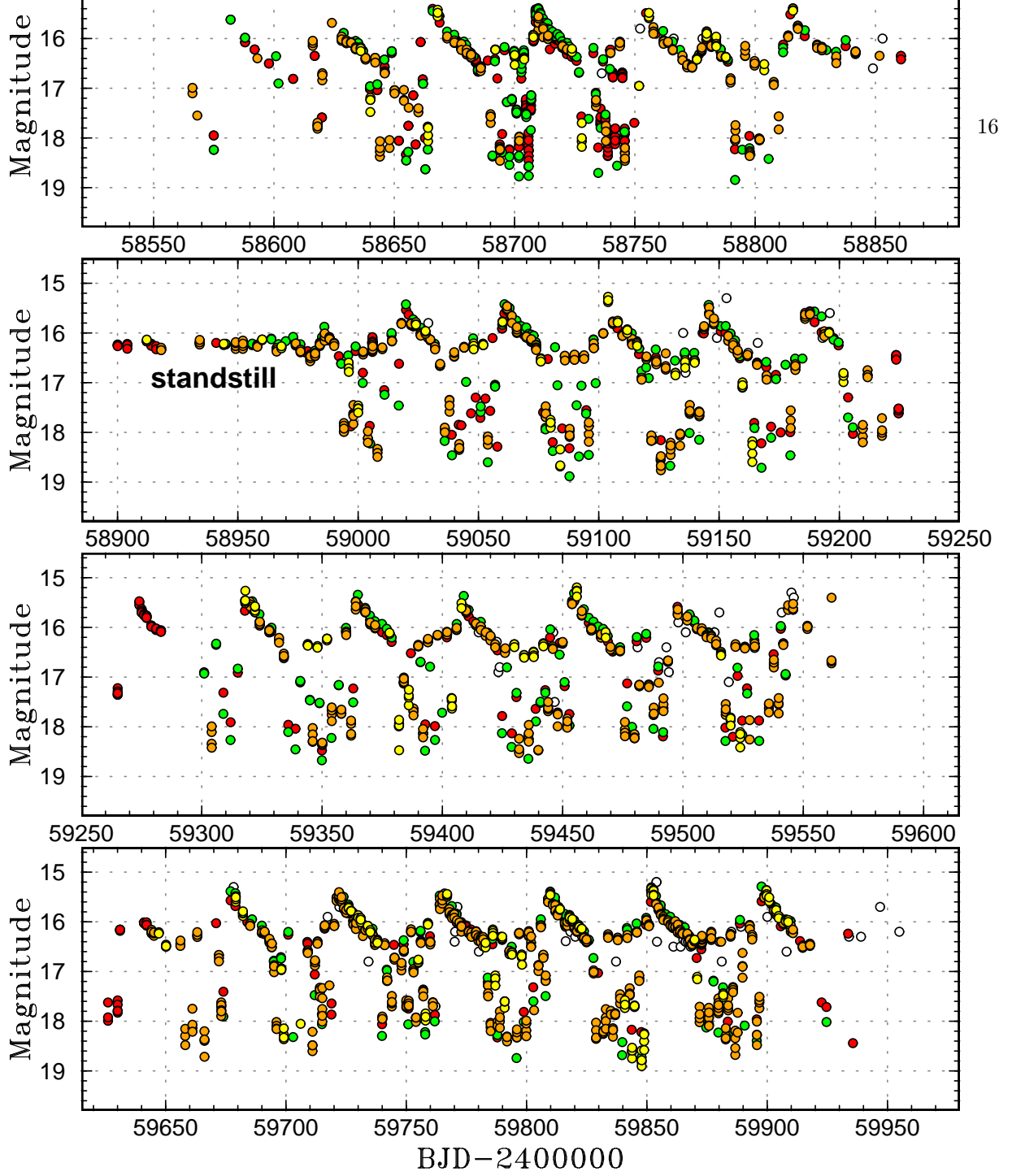


Figure 11: Light curve of DDE 48 in 2019–2022. The symbols are the same as in figure 10. There was a standstill between BJD 2458826 (2019 December 8) and BJD 2458993 (2020 May 23) (end of the first to the start of the second panels) in addition to ER UMA-type supercycles.

4.2 MGAB-V728

MGAB-V728 was discovered as a Z Cam star by G. Murawski in 2019.¹⁰ The ZTF light curve is shown in figure 12. A standstill was present in 2019. At other times, the object displayed ER UMa-type behavior. This object was also listed as a Gaia variable Gaia DR3 4530506601048215296 (type CV) (Gaia Collaboration et al. 2022). Superhumps have not yet been confirmed.

4.3 MGAB-V3488

This object was originally selected as a candidate RR Lyr star (PS1-3PI J045544.81+653834.2: Sesar et al. 2017). G. Murawski (MGAB-V3488¹¹ reported it to be a Z Cam star. M. Bajer also reported its variability (BMAM-V809). The object was identified as an ER UMa star with a short supercycle (~ 25 d) comparable to RZ LMi (T. Kato, vsnet-chat 8778¹²). The ZTF light curve is shown in figure 13. The object was in standstill at least up to 2019 April. The object showed an ER UMa-type supercycle between BJD 2458694 (2019 July 29) and 2458720 (2019 August 24); normal outbursts were not recorded due to the sparse coverage, then entered a standstill again. This standstill ended by fading (BJD 2458903 = 2020 February 24). In 2020–2022, the object was mostly in ER UMa states with short (~ 25 d) supercycles. There was a possible standstill around BJD 2459777 (2022 July 16) to BJD 2459783 (2022 July 22), which was not well covered by observations. The ER UMa-type classification of the object was confirmed by the presence of short outbursts between longer ones (superoutbursts). Superhumps have not yet been confirmed.

4.4 PS1-3PI J181732.65+101954.6

This object was selected as a candidate RR Lyr star (Sesar et al. 2017). T. Kato found it to be a dwarf nova (vsnet-chat 8487¹³). It was originally considered as an SS Cyg star, but later found to be an ER UMa star which entered a standstill in 2020 May (T. Kato, vsnet-alert 26776¹⁴). The ZTF light curve is shown in figure 14. As stated in vsnet-alert 26776, the behavior in 2018 (at least up to BJD 2458358 = 2018 August 27) was atypical and looked like repetitive rising standstills followed by dips, which are characteristics of an IW And star (Kato 2019). Although there were time-resolved ZTF data during one of brightening in 2018 (BJD 2458333–2458334 = 2018 August 3–4), regular superhumps were not recorded. We therefore consider that the behavior in 2018 was not a variety of superoutbursts in an ER UMa star. The behavior, however, did not perfectly match that of a typical IW And star in that it did not show brightening just before a dip. There was a superoutburst in 2019 June–July, which was not clearly preceded by a dwarf nova state and it looked like brightening from a plateau phase of the preceding outburst. Superhumps were recorded during this 2019 June–July outburst by ZTF time-resolved photometry (figure 15). The mean superhump period during this interval was 0.08879(2) d. This object is also known as BMAM-V769 (M. Bajer)¹⁵ and ZTF J181732.64+101954.5 (Ofek et al. 2020).

4.5 ZTF18abmpkbj

This object was originally selected as a candidate RR Lyr star (PS1-3PI J202831.22+200027.3) (Sesar et al. 2017). The object was found to be an ER UMa star (T. Kato, vsnet-chat 8649¹⁶). The classification was updated later (T. Kato, vsnet-chat 9037¹⁷) based on a standstill starting in 2021 September. This object was listed as a variable star ZTF J202831.22+200027.2 (Ofek et al. 2020). The ZTF light curve is shown in figure 16. In addition to ER UMa states, two standstills in 2018 and 2021 September–November were present. The ER UMa-type supercycle starting on BJD 2458664 (2019 June 29) had many normal outbursts between the superoutbursts and the supercycle was long (71 d). The behavior became more regular between BJD 2459052 (2020 July 21) and 2459411 (2021 July 15) showing typical ER UMa-type supercycles with 42–56 d. More variations were recorded during the 2021 standstill than in the 2018 one and the former may have shown weak dwarf nova-type outbursts

¹⁰<https://sites.google.com/view/mgab-astronomy/mgab-v701-v750>. This page has been updated after the initial submission to the AAVSO VSX (Watson et al. 2006).

¹¹<https://sites.google.com/view/mgab-astronomy/mgab-v3451-v3500>.

¹²<http://ooruri.kusastro.kyoto-u.ac.jp/mailarchive/vsnet-chat/8778>.

¹³<http://ooruri.kusastro.kyoto-u.ac.jp/mailarchive/vsnet-chat/8487>.

¹⁴<http://ooruri.kusastro.kyoto-u.ac.jp/mailarchive/vsnet-alert/26776>.

¹⁵https://www.aavso.org/vsx_docs/2213875/3635/BMAM-V769%20light%20curve.PNG.

¹⁶<http://ooruri.kusastro.kyoto-u.ac.jp/mailarchive/vsnet-chat/8649>.

¹⁷<http://ooruri.kusastro.kyoto-u.ac.jp/mailarchive/vsnet-chat/9037>.

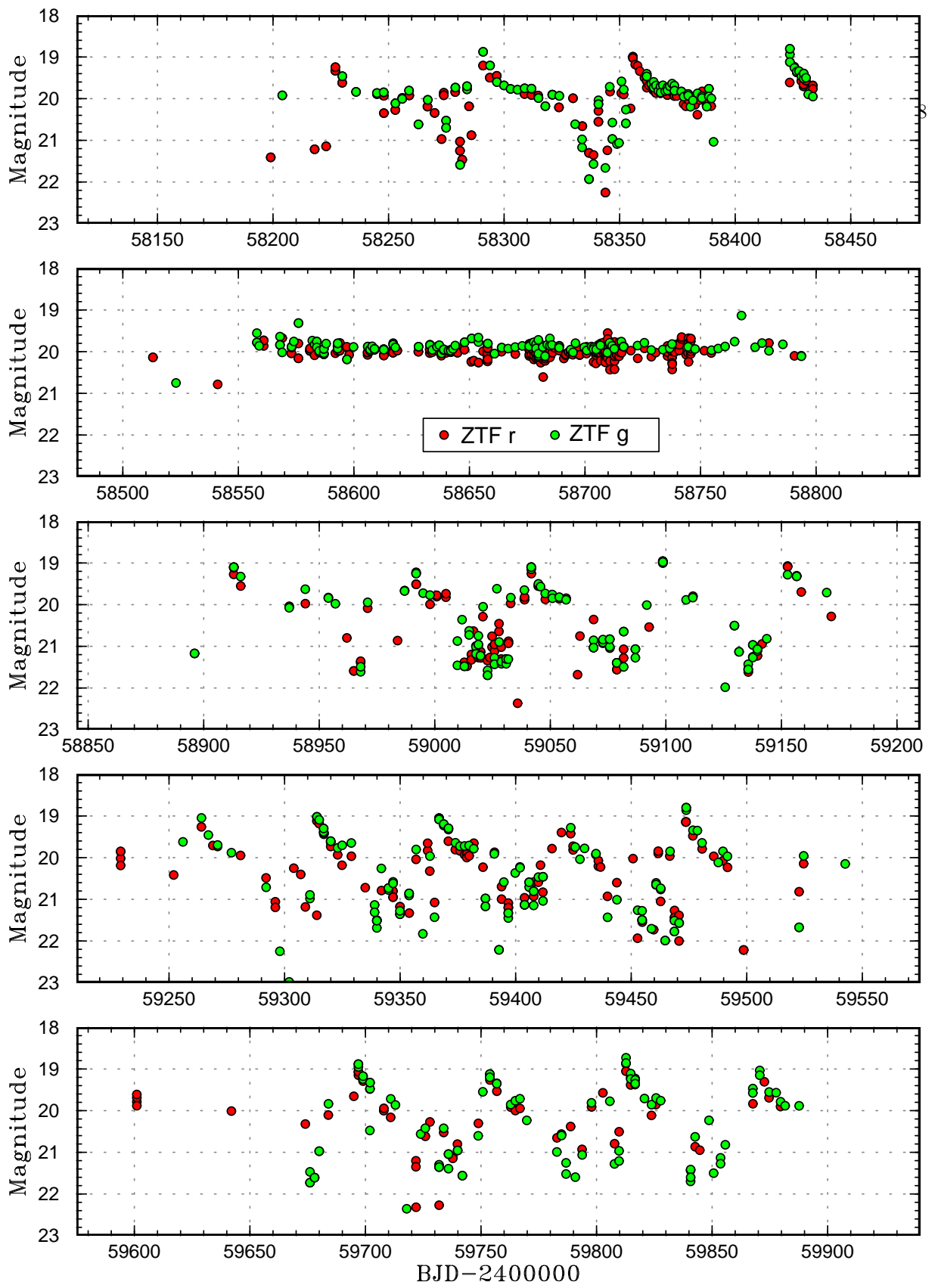


Figure 12: Light curve of MGAB-V728 in 2018–2022. The object showed ER UMa-type supercycles except a standstill in 2019 (second panel).

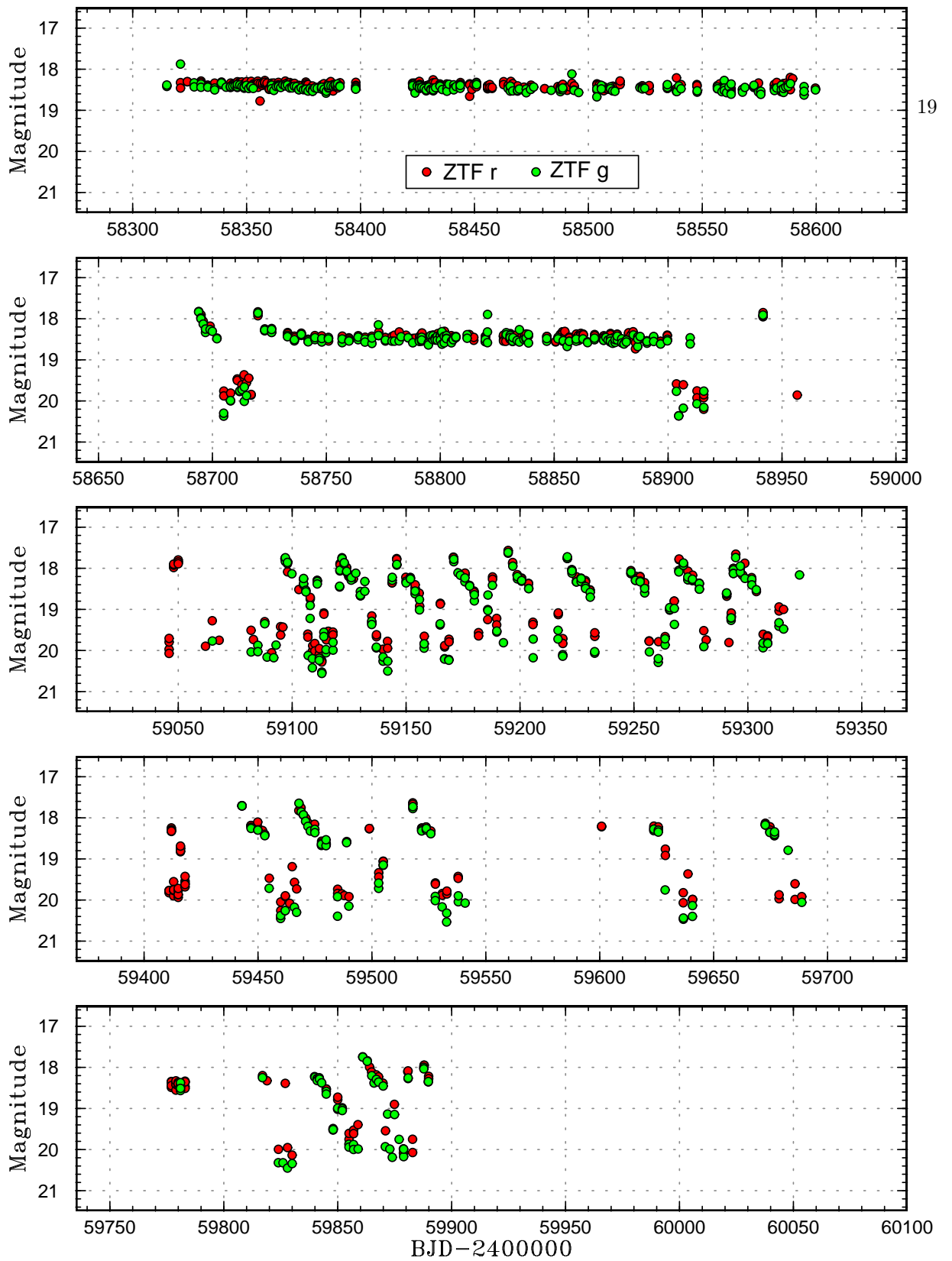


Figure 13: Light curve of MGAB-V3488 in 2018–2022. The object was in standstill at least up to 2019 April (first panel). The object showed an ER Uma-type supercycle between BJD 2458694 (2019 July 29) and 2458720 (2019 August 24) (second panel), then entered a standstill again. In 2020–2022, the object was mostly in ER Uma states with short (~ 25 d) supercycles.

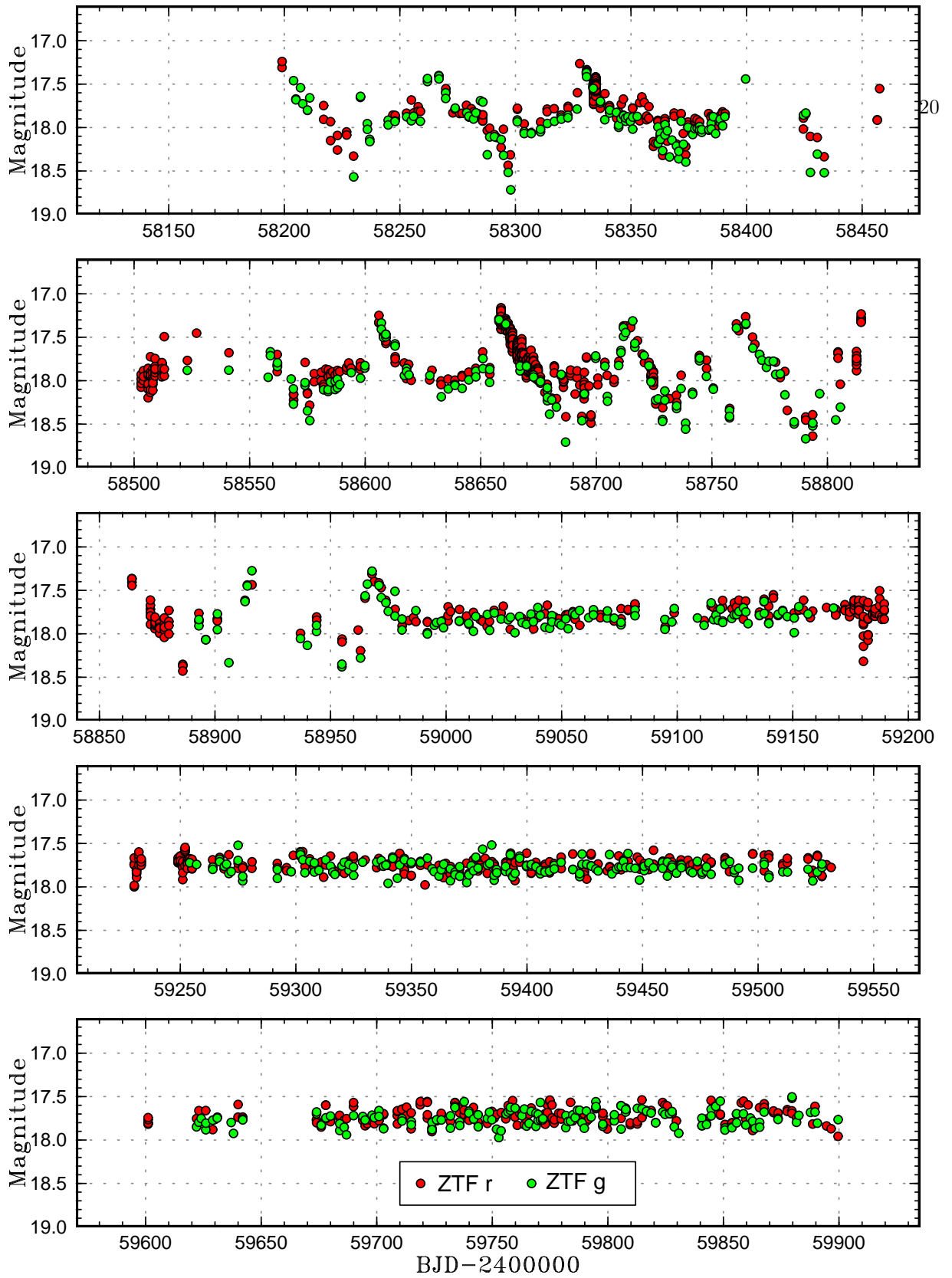


Figure 14: Light curve of PS1-3PI J181732.65+101954.6 in 2018–2022. The object was in an ER UMa state in 2019 to 2020 May (second and third panels), then entered a long standstill lasting up to now. The behavior in 2018 (first panel) was unusual and it looked like an IW And star (see text).

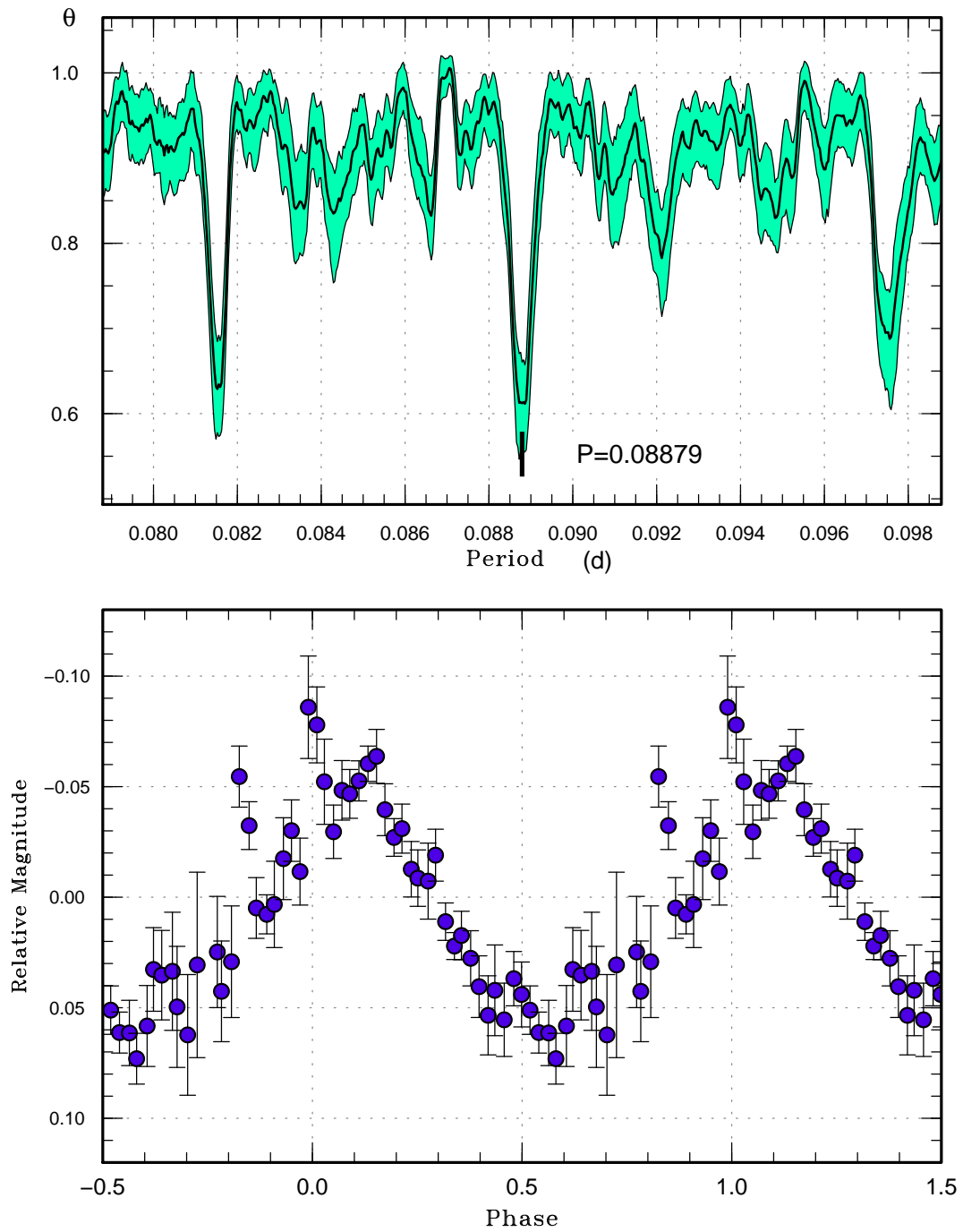


Figure 15: Mean superhump profile of PS1-3PI J181732.65+101954.6 from ZTF time-resolved data for BJD 2458657.8–2458674.8. (Upper): PDM analysis. See figure 6 for explanation. (Lower): Phase plot.

during the standstill. The object was again in a typical ER UMa state in 2022. Superhumps have not yet been confirmed.

4.6 ZTF18abncpgs

This object was originally selected as a candidate RR Lyr star (PS1-3PI J005932.18+570342.7) (Sesar et al. 2017). AAVSO VSX (Watson et al. 2006) listed the object as a Z Cam star in 2021. T. Kato (vsnet-chat 8896¹⁸) noted that this object is similar to the ER UMa star RZ LMi with variable supercycles in addition to a standstill. The ZTF light curve is shown in figure 17. Since 2019, the object stayed in standstill much of the time while there were occasional ER UMa states. In 2018, this object was apparently in an ER UMa state with a mean supercycle of ~ 52 d. The superoutburst starting on BJD 2458672 (2019 July 19) showed brightening in the later phase. The next superoutburst had a long plateau (or a short standstill) as seen in RZ LMi (Kato et al. 2016). The later standstill after 2020 May was interrupted by one or two ER UMa-type dwarf nova cycles. This object is also known as ATO J014.8840+57.0618 (Heinze et al. 2018) and ZTF J005932.18+570342.7 (Ofek et al. 2020). Superhumps have not yet been confirmed.

4.7 ZTF19aarsljl

This object was originally selected as a candidate RR Lyr star (PS1-3PI J084907.10–152526.7) (Sesar et al. 2017). T. Kato (vsnet-chat 9068¹⁹) noted that this object is likely an ER UMa star with standstills. The ZTF light curve is shown in figure 18. The part BJD 2459155 (2020 November 4) to BJD 2459304 (2021 March 30) looks like an extended superoutburst followed by dwarf nova outbursts as in RZ LMi (Kato et al. 2016). The short cycle between BJD 2458800 (2019 November 12) and 2458880 (2020 January 31) suggests an ER UMa-type object. The segment between BJD 2458424 (2018 November 1) and 2458560 (2019 March 18) was apparently a standstill. Although the quality of the data was not sufficient due to the faintness of the object and the short coverage by ZTF, we consider that this object is an ER UMa star close to the thermal stability as in RZ LMi when it showed standstills. This object was also listed as a Gaia variable Gaia DR3 5733518178924667392 (type CV) (Gaia Collaboration et al. 2022). Superhumps have not yet been confirmed.

4.8 MGAB-V284

This object was reported as a Z Cam star by G. Murawski.²⁰ T. Kato pointed out in vsnet-alert 23716²¹ as follows (typos corrected): “According to ZTF data, a large and long outburst triggered a standstill. The outburst amplitudes between the standstills gradually grew up. While the outburst amplitude just after the end of the standstill is 2.5 mag and the duration is 3 d, the outburst amplitude just before the standstill is 3.5 mag and the duration is 20 d. In addition, recurrence time might be 120 d according to Apparent Magnitude on Lasair data (<https://lasair.roe.ac.uk/object/ZTF18abgpmcd/>)”. This statement was based on ZTF Lasair data (Smith et al. 2019) and is updated here using the most recent release of the ZTF data (figure 19). All “outbursts” occurred after a sequence of short-period dwarf nova oscillations and the behavior is most analogous to ER UMa stars with long standstills, such as ZTF18abncpgs. The only difference is in the time scale: the cycle lengths of normal outbursts are ~ 10 d compared to ~ 4 d in ER UMa stars. This difference implies that the orbital period is longer than those of typical ER UMa stars. In recent years, however, a number of SU UMa stars above the period gap have been identified, breaking the general consensus (Warner 1995) such as BO Cet (Kato et al. 2021; Kato 2023a), MisV1448 (N. Kojiguchi et al. in preparation), ASASSN-18aan (Wakamatsu et al. 2021) and ASASSN-15cm (Kato 2023b), and MGAB-V284 may be an ER UMa star with standstills above the period gap. Although the period was not determined due to the very small number of observations, the large scatter in the ZTF light curve around the peak of the 2018 October outburst was suggestive of superhumps (figure 20). Further observations around the peak of a future bright outburst are requested. This object is also known as ZTF J221257.97+490644.4 (Ofek et al. 2020) and was also listed as a Gaia variable Gaia DR3 1975922107078810112 (type CV) (Gaia Collaboration et al. 2022).

¹⁸<http://ooruri.kusastro.kyoto-u.ac.jp/mailarchive/vsnet-chat/8896>.

¹⁹<http://ooruri.kusastro.kyoto-u.ac.jp/mailarchive/vsnet-chat/9068>.

²⁰https://www.aavso.org/vsx_docs/844556/3120/MGAB-V284.png.

²¹<http://ooruri.kusastro.kyoto-u.ac.jp/mailarchive/vsnet-alert/23716>.

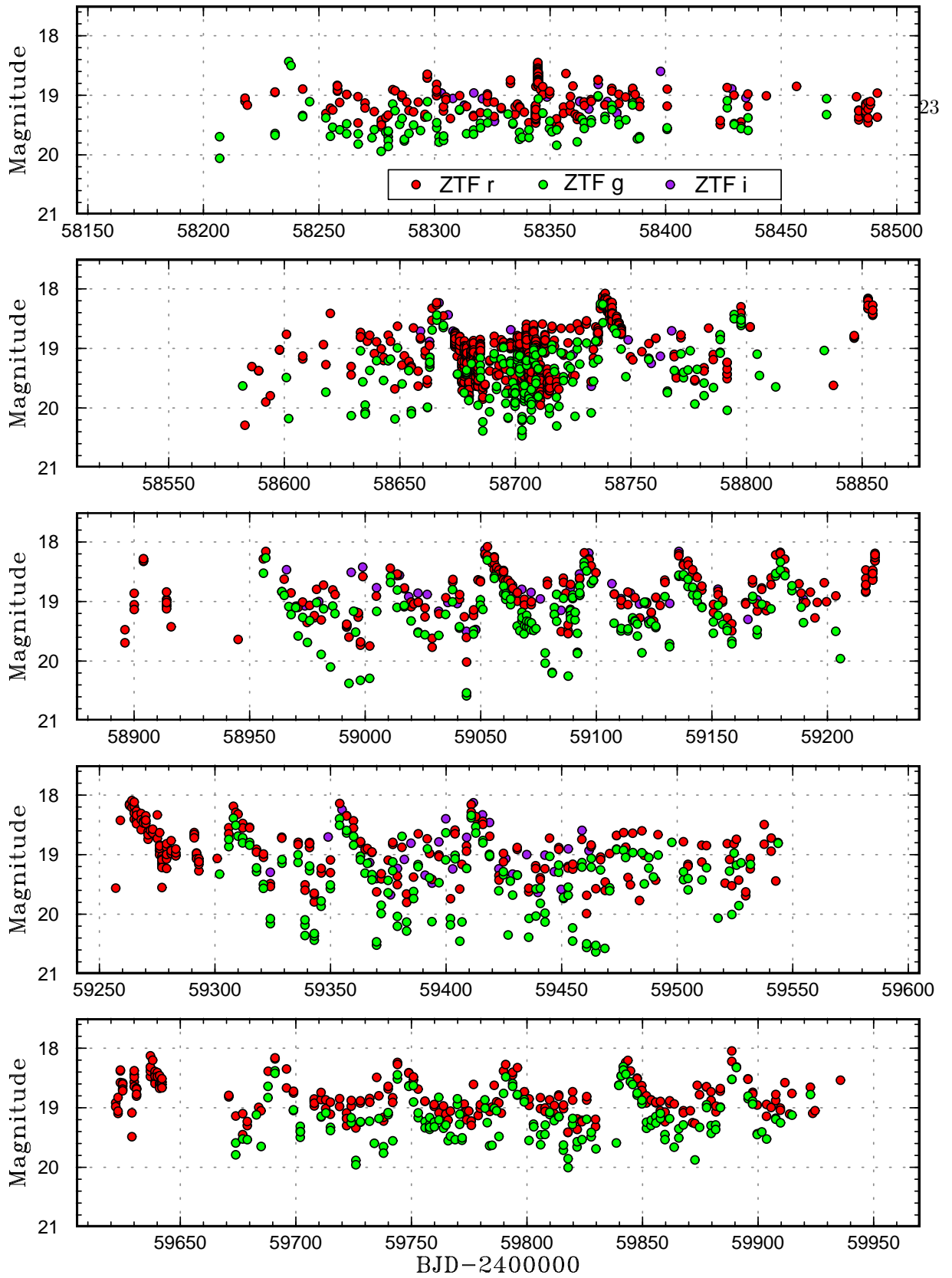


Figure 16: Light curve of ZTF18abmpkbj in 2018–2022. In addition to ER UMa states, two standstills in 2018 (first panel) and 2021 September–November (fourth panel) were present.

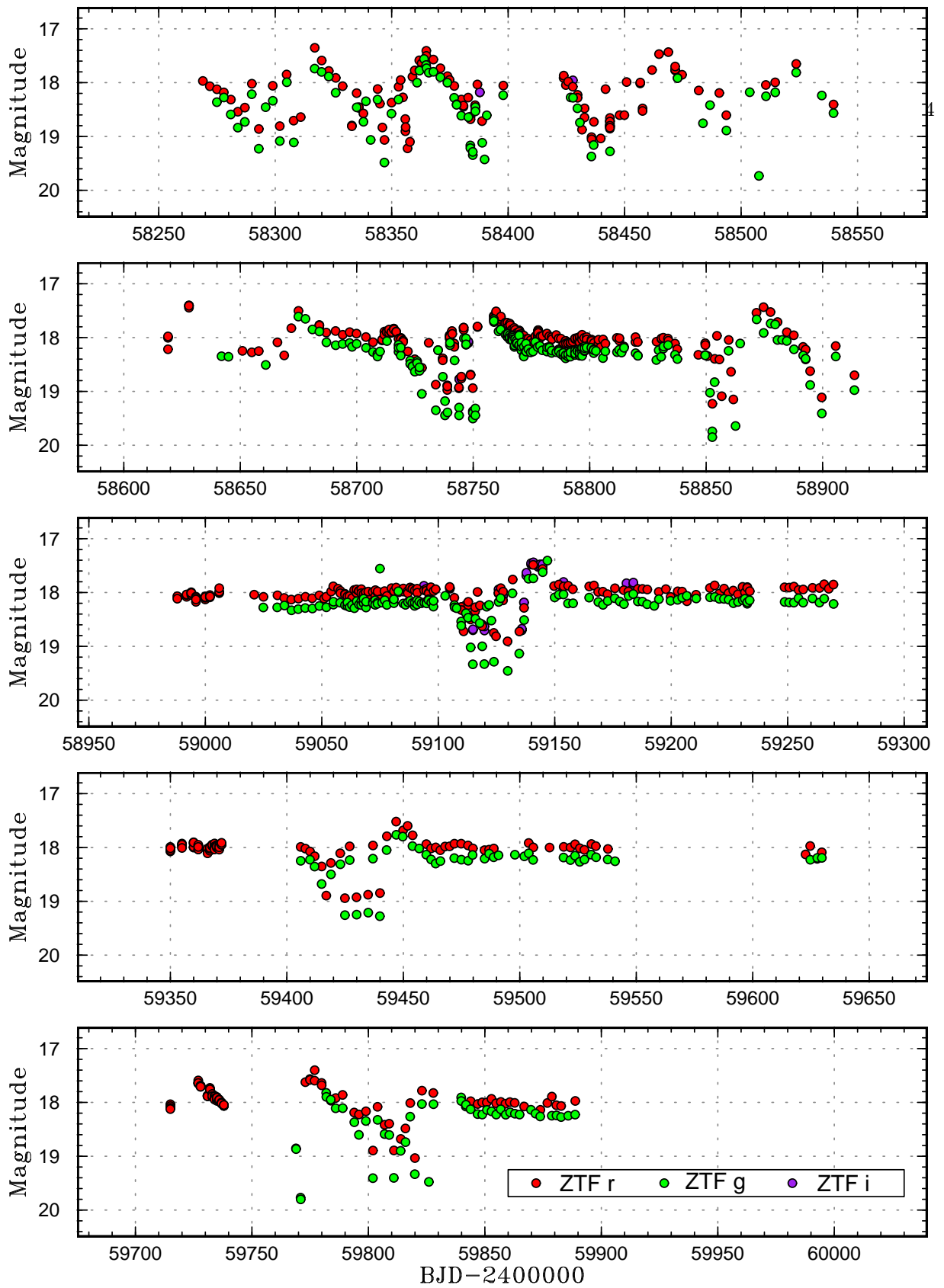


Figure 17: Light curve of ZTF18abncpgs in 2018–2022. Since 2019, the object stayed in standstill much of the time while there were occasional ER UMA states.

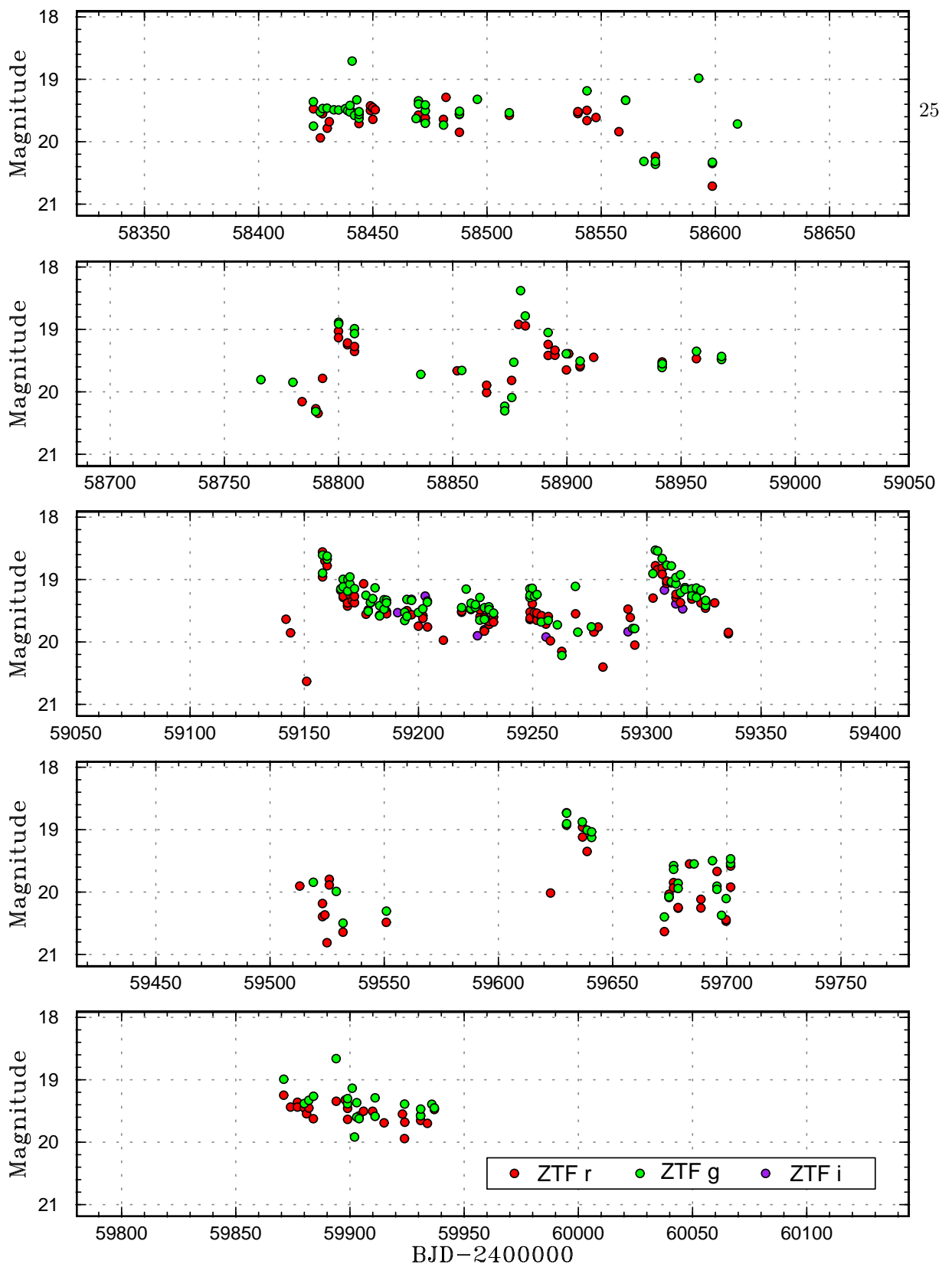


Figure 18: Light curve of ZTF19aarsljl in 2018–2022. The part BJD 2459155 (2020 November 4) to BJD 2459304 (2021 March 30, third panel) looks like an extended superoutburst followed by dwarf nova outbursts as in RZ LMi (Kato et al. 2016). The short cycle between BJD 2458800 (2019 November 12) and 2458880 (2020 January 31, second panel) suggests an ER UMa-type object. The segment between BJD 2458424 (2018 November 1) and 2458560 (2019 March 18, first panel) was apparently a standstill.

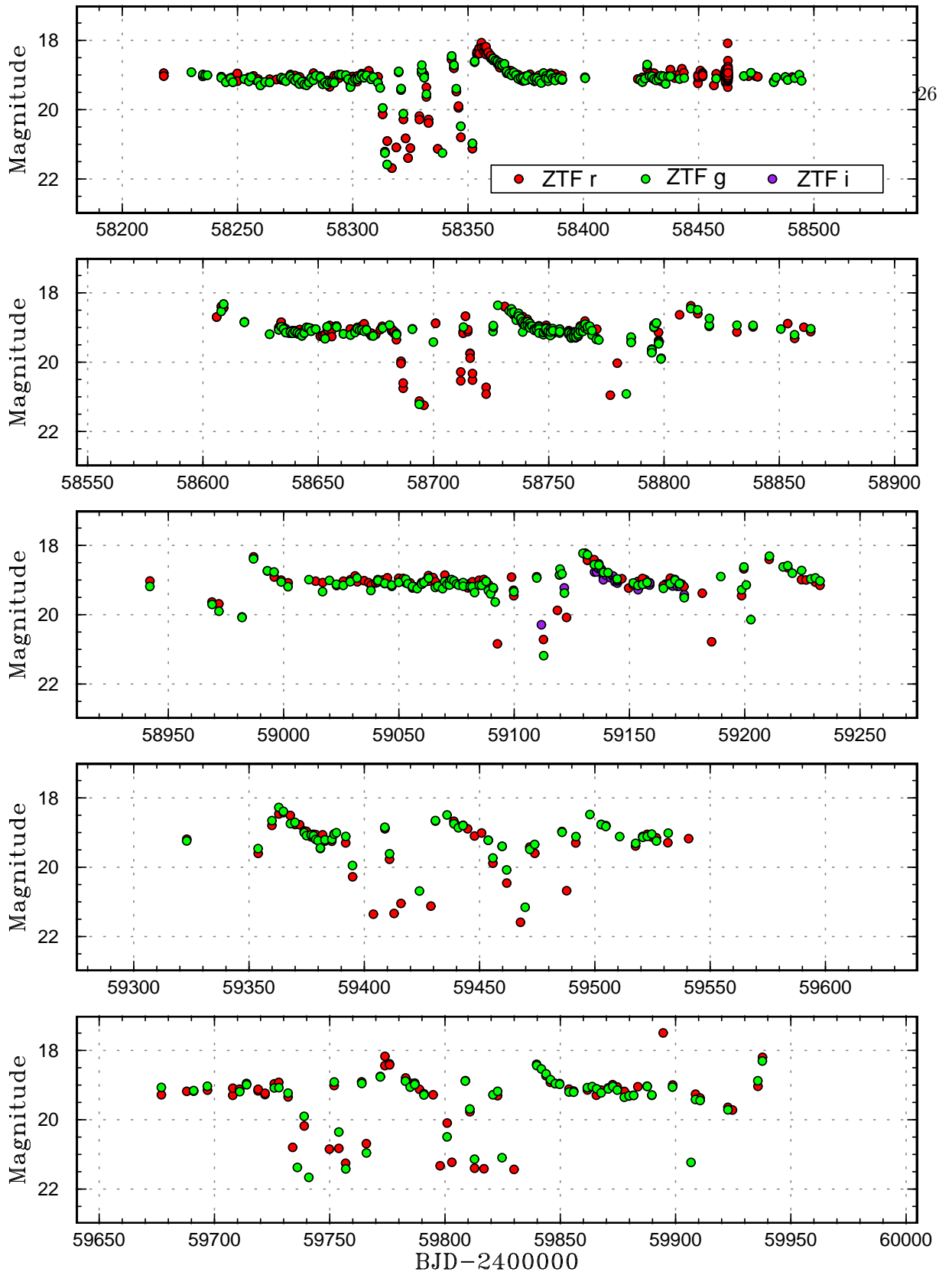


Figure 19: Light curve of MGAB-V284 in 2018–2022.

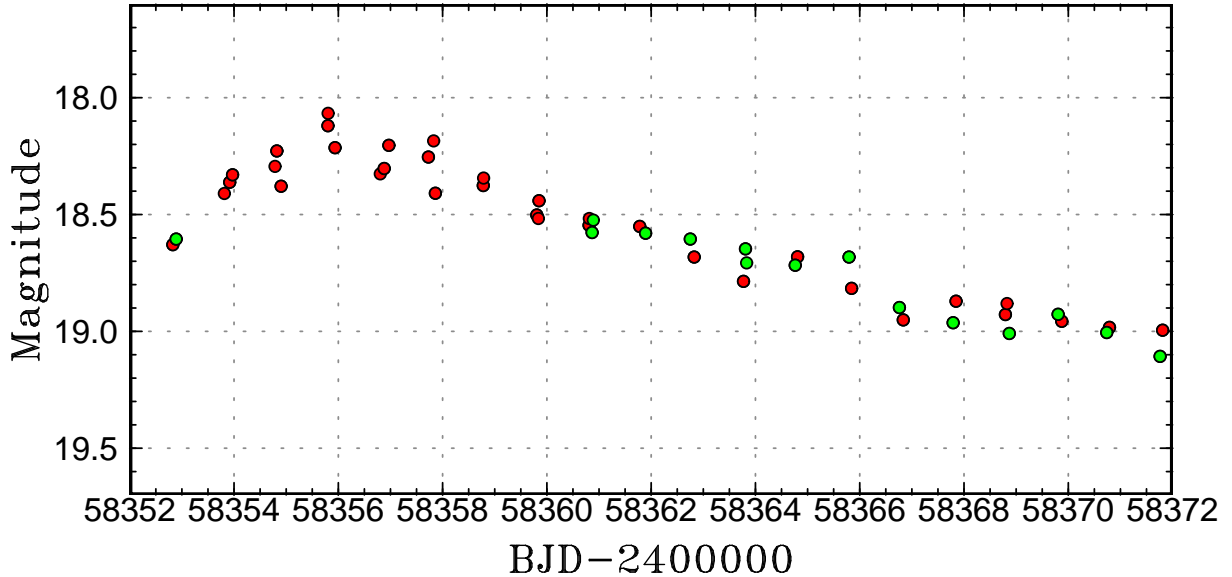


Figure 20: Light curve of MGAB-V284 around the peak of the 2018 October outburst. The symbols are the same as in figure 19.

5 Summary

We analyzed ASAS-SN, ATLAS and TESS observations of CM Mic and found that this object belongs to a small group of ER UMa stars showing standstills. The object showed typical ER UMa-type cycles between 2019 July and 2021 November, and in 2023. It showed standstills between 2017 and 2019 July, and in 2022. The supercycles varied between 49 and 83 d, which probably reflected the variable mass-transfer rate. In 2015, the object showed outbursts with a cycle length of ~ 35 d in 2015 whose variations became weaker in 2016. An analysis of TESS observations during the 2020 July outburst detected superhumps with a mean period of $0.080251(6)$ d (value after the full development of superhumps). and a period of the growing stage of $0.0817(2)$ d. The period derivative $+2.0(2) \times 10^{-5}$ was similar to those recorded in other ER UMa stars.

We also studied previously undocumented ER UMa stars showing standstills mainly using ZTF data.

- DDE 48 mostly showed ER UMa-type supercycles but showed a standstill in 2019 December–2020 May. MGAB-V728 also mostly showed ER UMa-type supercycles but showed a standstill in 2019.
- MGAB-V3488 showed long standstills in 2018–2020, but was mostly in ER UMa states with short (~ 25 d) supercycles in 2020–2022 similar to RZ LMi.
- PS1-3PI J181732.65+101954.6 showed ER UMa-type supercycles up to 2020 May and entered a long standstill lasting up to now.
- ZTF18abmpkbj mostly showed ER UMa-type supercycles but two standstills were recorded in 2018 and late 2021. These standstills had larger variations than in other objects and this object may have shown weak dwarf nova-type outbursts during the standstills.
- ZTF18abncpgs showed standstills most of the time, but also showed ER UMa-type supercycles in 2018 and occasionally between standstills.
- ZTF19aarsljl is likely an ER UMa star with standstills, but the details were not clear due to the faintness.
- MGAB-V284 showed a pattern similar to ER UMa stars showing standstills but with a longer time-scale of normal outbursts. We suspect that this object is an ER UMa star with standstills above the period gap.

None of the objects we studied showed a superoutburst arising from a long standstill, as recorded in NY Ser in 2018, although the 2019 June–July superoutburst of PS1-3PI J181732.65+101954.6 may have directly occurred

without experiencing a dwarf nova state and it could have been analogous to a superoutburst arising from a standstill. The case of NY Ser appears to be very rare and we could not find additional evidence that the disk radius during standstills in ER UMa stars increases.

Acknowledgements

This work was supported by JSPS KAKENHI Grant Number 21K03616. The authors are grateful to the ASAS-SN, ATLAS, TESS and ZTF teams for making their data available to the public. We are grateful to VSOLJ and VSNET observers (particularly M. Moriyama, G. Poyner, Y. Maeda and M. Hiraga) who reported snapshot CCD photometry of DDE 48.

Funding for the TESS mission is provided by the NASA Science Mission Directorate.

This work has made use of data from the Asteroid Terrestrial-impact Last Alert System (ATLAS) project. The ATLAS project is primarily funded to search for near earth asteroids through NASA grants NN12AR55G, 80NSSC18K0284, and 80NSSC18K1575; byproducts of the NEO search include images and catalogs from the survey area. This work was partially funded by Kepler/K2 grant J1944/80NSSC19K0112 and HST GO-15889, and STFC grants ST/T000198/1 and ST/S006109/1. The ATLAS science products have been made possible through the contributions of the University of Hawaii Institute for Astronomy, the Queen’s University Belfast, the Space Telescope Science Institute, the South African Astronomical Observatory, and The Millennium Institute of Astrophysics (MAS), Chile.

Based on observations obtained with the Samuel Oschin 48-inch Telescope at the Palomar Observatory as part of the Zwicky Transient Facility project. ZTF is supported by the National Science Foundation under Grant No. AST-1440341 and a collaboration including Caltech, IPAC, the Weizmann Institute for Science, the Oskar Klein Center at Stockholm University, the University of Maryland, the University of Washington, Deutsches Elektronen-Synchrotron and Humboldt University, Los Alamos National Laboratories, the TANGO Consortium of Taiwan, the University of Wisconsin at Milwaukee, and Lawrence Berkeley National Laboratories. Operations are conducted by COO, IPAC, and UW.

The ztfquery code was funded by the European Research Council (ERC) under the European Union’s Horizon 2020 research and innovation programme (grant agreement n°759194 – USNAC, PI: Rigault).

List of objects in this paper

CR Boo, Z Cam, BO Cet, AM CVn, SS Cyg, RZ LMi, BK Lyn, RR Lyr, CM Mic, NY Ser, SU UMa, ER UMa, ASASSN-15cm, ASASSN-18aan, ATO J014.8840+57.0618, ATO J311.5492+24.3492, BMAM-V769, BMAM-V809, DDE 48, EC 20335–4332, Gaia DR3 1843254106354614272, Gaia DR3 1975922107078810112, Gaia DR3 4530506601048215296, Gaia DR3 5733518178924667392, MGAB-V284, MGAB-V728, MGAB-V859, MGAB-V3488, MisV1448, PS1-3PI J005932.18+570342.7, PS1-3PI J045544.81+653834.2, PS1-3PI J084907.10–152526.7, PS1-3PI J181732.65+101954.6, PS1-3PI J202831.22+200027.3, PS1-3PI J204611.81+242057.2, WFI J161953.3+031909, ZTF18abgjsdg, ZTF18abmpkbj, ZTF18abncpgs, ZTF19aarsljl, ZTF J005932.18+570342.7, ZTF J181732.64+101954.5, ZTF J221257.97+490644.4

References

We provide two forms of the references section (for ADS and as published) so that the references can be easily incorporated into ADS.

References (for ADS)

- Beers, T. C., Preston, G. W., Shectman, S. A., Doinidis, S. P., & Griffin, K. E. (1992) Spectroscopy of hot stars in the Galactic halo. *AJ* **103**, 267
- Chen, A., O’Donoghue, D., Stobie, R. S., Kilkeny, D., & Warner, B. (2001) Cataclysmic variables in the Edinburgh-Cape Blue Object Survey. *MNRAS* **325**, 89

- Cleveland, W. S. (1979) Robust locally weighted regression and smoothing scatterplots. *J. Amer. Statist. Assoc.* **74**, 829
- Fernie, J. D. (1989) Uncertainties in period determinations. *PASP* **101**, 225
- Gaia Collaboration et al. (2022) Gaia Data Release 3. Summary of the contents and survey properties. *A&A* (arXiv:2208.00211)
- Heinze, A. N. et al. (2018) A first catalog of variable stars measured by the Asteroid Terrestrial-impact Last Alert System (ATLAS). *AJ* **156**, 241
- Kato, T., Nogami, D., & Masuda, S. (1996) Large-amplitude superhumps in ER Ursae Majoris during the earliest stage of a superoutburst. *PASJ* **48**, L5
- Kato, T. (2019) Three Z Cam-type dwarf novae exhibiting IW And-type phenomenon. *PASJ* **71**, 20
- Kato, T. (2022a) Evolution of short-period cataclysmic variables: implications from eclipse modeling and stage a superhump method (with New Year's gift). *VSOLJ Variable Star Bull.* **89**, (arXiv:2201.02945)
- Kato, T. (2022b) WFI J161953.3+031909: eclipsing ER UMa-type and Z Cam-type star in the period gap. *VSOLJ Variable Star Bull.* **96**, (arXiv:2203.06785)
- Kato, T. (2022c) Analysis of TESS observations of V844 Her during the 2020 superoutburst. *VSOLJ Variable Star Bull.* **102**, (arXiv:2205.05284)
- Kato, T. (2023a) SU UMa-type supercycle in the IW And-type dwarf nova BO Cet above the period gap. *VSOLJ Variable Star Bull.* **106**, (arXiv:2302.02593)
- Kato, T. (2023b) ASASSN-15cm: an SU UMa star with an orbital period of 5.0 hours. *VSOLJ Variable Star Bull.* **109**, (arXiv:2302.09713)
- Kato, T. et al. (2013) Survey of period variations of superhumps in SU UMa-type dwarf novae. IV: The fourth year (2011–2012). *PASJ* **65**, 23
- Kato, T. et al. (2009) Survey of period variations of superhumps in SU UMa-type dwarf novae. *PASJ* **61**, S395
- Kato, T. et al. (2016) RZ Leonis Minoris bridging between ER Ursae Majoris-type dwarf nova and nova-like system. *PASJ* **68**, 107
- Kato, T. et al. (2017) Survey of period variations of superhumps in SU UMa-type dwarf novae. IX. The ninth year (2016–2017). *PASJ* **69**, 75
- Kato, T., & Kojiguchi, N. (2021) MGAB-V859 and ZTF18abgjsdg: ER UMa-type dwarf novae showing standstills. *VSOLJ Variable Star Bull.* **78**, (arXiv:2107.14400)
- Kato, T., & Kunjaya, C. (1995) Discovery of a peculiar SU UMa-type dwarf nova ER Ursae Majoris. *PASJ* **47**, 163
- Kato, T., Maeda, Y., & Moriyama, M. (2023) Genuine standstill in the AM CVn star CR Boo. *VSOLJ Variable Star Bull.* **107**, (arXiv:2302.04454)
- Kato, T. et al. (2010) Survey of period variations of superhumps in SU UMa-type dwarf novae. II. The second year (2009–2010). *PASJ* **62**, 1525
- Kato, T., Nogami, D., Baba, H., Masuda, S., Matsumoto, K., & Kunjaya, C. (1999) in *Disk Instabilities in Close Binary Systems*, ed. S. Mineshige, & J. C. Wheeler (Tokyo: Universal Academy Press) p. 45
- Kato, T., Nogami, D., & Masuda, S. (2003) Unusual phase reversal of superhumps in ER Ursae Majoris. *PASJ* **55**, L7
- Kato, T., & Osaki, Y. (2013) New method to estimate binary mass ratios by using superhumps. *PASJ* **65**, 115
- Kato, T. et al. (2019) Discovery of standstills in the SU UMa-type dwarf nova NY Serpentis. *PASJ* **71**, L1

- Kato, T. et al. (2021) BO Ceti: Dwarf nova showing both IW And and SU UMa-type features. *PASJ* **73**, 1280
- Kazarovets, E. V., Kireeva, N. N., Samus, N. N., & Durlevich, O. V. (2003) The 77th name-list of variable stars. *IBVS* **5422**, 1
- Kemp, J. et al. (2012) in Proc. 31st Annu. Conf., Symp. on Telescope Science, ed. B. D. Warner, & et al. (Rancho Cucamonga: Society for Astronomical Sciences) p. 7
- Kimura, M., Osaki, Y., Kato, T., & Mineshige, S. (2020) Thermal-viscous instability in tilted accretion disks: A possible application to IW Andromeda-type dwarf novae. *PASJ* **72**, 22
- Kochanek, C. S. et al. (2017) The All-Sky Automated Survey for Supernovae (ASAS-SN) light curve server v1.0. *PASP* **129**, 104502
- Masci, F.-J. et al. (2019) The Zwicky Transient Facility: Data processing, products, and archive. *PASP* **131**, 018003
- Nogami, D., Kato, T., Baba, H., & Masuda, S. (1998) Discovery of the first in-the-gap SU UMa-type dwarf nova, NY Serpentis (=PG 1510+234). *PASJ* **50**, L1
- Ofek, E. O., Soumagnac, M., Nir, G., Gal-Yam, A., Nugent, P., Masci, F., & Kulkarni, S. R. (2020) A catalogue of over 10 million variable source candidates in ZTF Data Release 1. *MNRAS* **499**, 5782
- Ohshima, T. et al. (2014) Study of negative and positive superhumps in ER Ursae Majoris. *PASJ* **66**, 67
- Osaki, Y. (1995) A model for a peculiar SU Ursae Majoris-type dwarf nova ER Ursae Majoris. *PASJ* **47**, L11
- Osaki, Y. (1996) Dwarf-nova outbursts. *PASP* **108**, 39
- Patterson, J., Jablonski, F., Koen, C., O'Donoghue, D., & Skillman, D. R. (1995) Superhumps in cataclysmic binaries. VIII. V1159 Orionis. *PASP* **107**, 1183
- Patterson, J. et al. (2013) BK Lyncis: the oldest old nova and a bellwether for cataclysmic variable evolution. *MNRAS* **434**, 1902
- Pavlenko, E. P. et al. (2014) NY Serpentis: SU UMa-type nova in the period gap with diversity of normal outbursts. *PASJ* **66**, 111
- Ricker, G. R. et al. (2015) Transiting Exoplanet Survey Satellite (TESS). *J. of Astron. Telescopes, Instruments, and Systems* **1**, 014003
- Ringwald, F. A., Thorstensen, J. R., Honeycutt, R. K., & Robertson, J. W. (1996) The orbital period of BK Lyncis (PG 0917+342). *MNRAS* **278**, 125
- Ritter, H., & Kolb, U. (2003) Catalogue of cataclysmic binaries, low-mass X-ray binaries and related objects (Seventh edition). *A&A* **404**, 301
- Robertson, J. W., Honeycutt, R. K., & Turner, G. W. (1995) RZ Leonis Minoris, PG 0943+521, and V1159 Orionis: Three cataclysmic variables with similar and unusual outburst behavior. *PASP* **107**, 443
- Sesar, B. et al. (2017) Machine-learned identification of RR Lyrae stars from sparse, multi-band data: The PS1 sample. *AJ* **153**, 204
- Shappee, B. J. et al. (2014) The man behind the curtain: X-rays drive the UV through NIR variability in the 2013 AGN outburst in NGC 2617. *ApJ* **788**, 48
- Shingles, L. et al. (2021) Release of the ATLAS Forced Photometry server for public use. *Transient Name Server AstroNote* **7**, 1
- Skillman, D. R., & Patterson, J. (1993) Superhumps in cataclysmic binaries. II. PG 0917+342. *ApJ* **417**, 298
- Sklyanov, A. S. et al. (2018) NY Ser: Outburst activity and multiperiodic processes in its various stages during 2014 and 2016. *Astrophysics* **61**, 64

- Smith, K. W. et al. (2019) Lasair: The transient alert broker for LSST:UK. *Research Notes of the American Astronom. Soc.* **3**, 26
- Stellingwerf, R. F. (1978) Period determination using phase dispersion minimization. *ApJ* **224**, 953
- Tonry, J. L. et al. (2018) ATLAS: A High-cadence All-sky Survey System. *PASP* **130**, 064505
- Wakamatsu, Y. et al. (2021) ASASSN-18aan: An eclipsing SU UMa-type cataclysmic variable with a 3.6-hr orbital period and a late G-type secondary star. *PASJ* **73**, 1209
- Warner, B. (1995) *Cataclysmic Variable Stars* (Cambridge: Cambridge University Press)
- Watson, C. L., Henden, A. A., & Price, A. (2006) The International Variable Star Index (VSX). *Society for Astronom. Sciences Ann. Symp.* **25**, 47
- Zemko, P., Kato, T., & Shugarov, S. Y. (2013) Detection of change in supercycles in ER Ursae Majoris. *PASJ* **65**, 54

References (as published)

- Beers, T. C., Preston, G. W., Shectman, S. A., Doinidis, S. P., & Griffin, K. E. (1992) Spectroscopy of hot stars in the Galactic halo. *AJ* **103**, 267
- Chen, A., O'Donoghue, D., Stobie, R. S., Kilkeny, D., & Warner, B. (2001) Cataclysmic variables in the Edinburgh-Cape Blue Object Survey. *MNRAS* **325**, 89
- Cleveland, W. S. (1979) Robust locally weighted regression and smoothing scatterplots. *J. Amer. Statist. Assoc.* **74**, 829
- Fernie, J. D. (1989) Uncertainties in period determinations. *PASP* **101**, 225
- Gaia Collaboration et al. (2022) Gaia Data Release 3. Summary of the contents and survey properties. *A&A* ([arXiv:2208.00211](https://arxiv.org/abs/2208.00211))
- Heinze, A. N. et al. (2018) A first catalog of variable stars measured by the Asteroid Terrestrial-impact Last Alert System (ATLAS). *AJ* **156**, 241
- Kato, T., Nogami, D., & Masuda, S. (1996) Large-amplitude superhumps in ER Ursae Majoris during the earliest stage of a superoutburst. *PASJ* **48**, L5
- Kato, T. (2019) Three Z Cam-type dwarf novae exhibiting IW And-type phenomenon. *PASJ* **71**, 20
- Kato, T. (2022a) Evolution of short-period cataclysmic variables: implications from eclipse modeling and stage a superhump method (with New Year's gift). *VSOLJ Variable Star Bull.* **89**, ([arXiv:2201.02945](https://arxiv.org/abs/2201.02945))
- Kato, T. (2022b) WFI J161953.3+031909: eclipsing ER UMa-type and Z Cam-type star in the period gap. *VSOLJ Variable Star Bull.* **96**, ([arXiv:2203.06785](https://arxiv.org/abs/2203.06785))
- Kato, T. (2022c) Analysis of TESS observations of V844 Her during the 2020 superoutburst. *VSOLJ Variable Star Bull.* **102**, ([arXiv:2205.05284](https://arxiv.org/abs/2205.05284))
- Kato, T. (2023a) SU UMa-type supercycle in the IW And-type dwarf nova BO Cet above the period gap. *VSOLJ Variable Star Bull.* **106**, ([arXiv:2302.02593](https://arxiv.org/abs/2302.02593))
- Kato, T. (2023b) ASASSN-15cm: an SU UMa star with an orbital period of 5.0 hours. *VSOLJ Variable Star Bull.* **109**, ([arXiv:2302.09713](https://arxiv.org/abs/2302.09713))
- Kato, T. et al. (2013) Survey of period variations of superhumps in SU UMa-type dwarf novae. IV: The fourth year (2011–2012). *PASJ* **65**, 23
- Kato, T. et al. (2009) Survey of period variations of superhumps in SU UMa-type dwarf novae. *PASJ* **61**, S395

- Kato, T. et al. (2016) RZ Leonis Minoris bridging between ER Ursae Majoris-type dwarf nova and nova-like system. *PASJ* **68**, 107
- Kato, T. et al. (2017) Survey of period variations of superhumps in SU UMa-type dwarf novae. IX. The ninth year (2016-2017). *PASJ* **69**, 75
- Kato, T., & Kojiguchi, N. (2021) MGAB-V859 and ZTF18abgjsdg: ER UMa-type dwarf novae showing standstills. *VSOLJ Variable Star Bull.* **78**, (arXiv:2107.14400)
- Kato, T., & Kunjaya, C. (1995) Discovery of a peculiar SU UMa-type dwarf nova ER Ursae Majoris. *PASJ* **47**, 163
- Kato, T., Maeda, Y., & Moriyama, M. (2023) Genuine standstill in the AM CVn star CR Boo. *VSOLJ Variable Star Bull.* **107**, (arXiv:2302.04454)
- Kato, T. et al. (2010) Survey of period variations of superhumps in SU UMa-type dwarf novae. II. The second year (2009–2010). *PASJ* **62**, 1525
- Kato, T., Nogami, D., Baba, H., Masuda, S., Matsumoto, K., & Kunjaya, C. (1999) in *Disk Instabilities in Close Binary Systems*, ed. S. Mineshige, & J. C. Wheeler (Tokyo: Universal Academy Press) p. 45
- Kato, T., Nogami, D., & Masuda, S. (2003) Unusual phase reversal of superhumps in ER Ursae Majoris. *PASJ* **55**, L7
- Kato, T., & Osaki, Y. (2013) New method to estimate binary mass ratios by using superhumps. *PASJ* **65**, 115
- Kato, T. et al. (2019) Discovery of standstills in the SU UMa-type dwarf nova NY Serpentis. *PASJ* **71**, L1
- Kato, T. et al. (2021) BO Ceti: Dwarf nova showing both IW And and SU UMa-type features. *PASJ* **73**, 1280
- Kazarovets, E. V., Kireeva, N. N., Samus, N. N., & Durlevich, O. V. (2003) The 77th name-list of variable stars. *IBVS* **5422**, 1
- Kemp, J. et al. (2012) in *Proc. 31st Annu. Conf., Symp. on Telescope Science*, ed. B. D. Warner, & et al. (Rancho Cucamonga: Society for Astronomical Sciences) p. 7
- Kimura, M., Osaki, Y., Kato, T., & Mineshige, S. (2020) Thermal-viscous instability in tilted accretion disks: A possible application to IW Andromeda-type dwarf novae. *PASJ* **72**, 22
- Kochanek, C. S. et al. (2017) The All-Sky Automated Survey for Supernovae (ASAS-SN) light curve server v1.0. *PASP* **129**, 104502
- Masci, F.-J. et al. (2019) The Zwicky Transient Facility: Data processing, products, and archive. *PASP* **131**, 018003
- Nogami, D., Kato, T., Baba, H., & Masuda, S. (1998) Discovery of the first in-the-gap SU UMa-type dwarf nova, NY Serpentis (=PG 1510+234). *PASJ* **50**, L1
- Ofek, E. O., Soumagnac, M., Nir, G., Gal-Yam, A., Nugent, P., Masci, F., & Kulkarni, S. R. (2020) A catalogue of over 10 million variable source candidates in ZTF Data Release 1. *MNRAS* **499**, 5782
- Ohshima, T. et al. (2014) Study of negative and positive superhumps in ER Ursae Majoris. *PASJ* **66**, 67
- Osaki, Y. (1995) A model for a peculiar SU Ursae Majoris-type dwarf nova ER Ursae Majoris. *PASJ* **47**, L11
- Osaki, Y. (1996) Dwarf-nova outbursts. *PASP* **108**, 39
- Patterson, J., Jablonski, F., Koen, C., O'Donoghue, D., & Skillman, D. R. (1995) Superhumps in cataclysmic binaries. VIII. V1159 Orionis. *PASP* **107**, 1183
- Patterson, J. et al. (2013) BK Lyncis: the oldest old nova and a bellwether for cataclysmic variable evolution. *MNRAS* **434**, 1902

- Pavlenko, E. P. et al. (2014) NY Serpentis: SU UMa-type nova in the period gap with diversity of normal outbursts. *PASJ* **66**, 111
- Ricker, G. R. et al. (2015) Transiting Exoplanet Survey Satellite (TESS). *J. of Astron. Telescopes, Instruments, and Systems* **1**, 014003
- Ringwald, F. A., Thorstensen, J. R., Honeycutt, R. K., & Robertson, J. W. (1996) The orbital period of BK Lyncis (PG 0917+342). *MNRAS* **278**, 125
- Ritter, H., & Kolb, U. (2003) Catalogue of cataclysmic binaries, low-mass X-ray binaries and related objects (Seventh edition). *A&A* **404**, 301
- Robertson, J. W., Honeycutt, R. K., & Turner, G. W. (1995) RZ Leonis Minoris, PG 0943+521, and V1159 Orionis: Three cataclysmic variables with similar and unusual outburst behavior. *PASP* **107**, 443
- Sesar, B. et al. (2017) Machine-learned identification of RR Lyrae stars from sparse, multi-band data: The PS1 sample. *AJ* **153**, 204
- Shappee, B. J. et al. (2014) The man behind the curtain: X-rays drive the UV through NIR variability in the 2013 AGN outburst in NGC 2617. *ApJ* **788**, 48
- Shingles, L. et al. (2021) Release of the ATLAS Forced Photometry server for public use. *Transient Name Server AstroNote* **7**, 1
- Skillman, D. R., & Patterson, J. (1993) Superhumps in cataclysmic binaries. II. PG 0917+342. *ApJ* **417**, 298
- Sklyanov, A. S. et al. (2018) NY Ser: Outburst activity and multiperiodic processes in its various stages during 2014 and 2016. *Astrophysics* **61**, 64
- Smith, K. W. et al. (2019) Lasair: The transient alert broker for LSST:UK. *Research Notes of the American Astronom. Soc.* **3**, 26
- Stellingwerf, R. F. (1978) Period determination using phase dispersion minimization. *ApJ* **224**, 953
- Tonry, J. L. et al. (2018) ATLAS: A High-cadence All-sky Survey System. *PASP* **130**, 064505
- Wakamatsu, Y. et al. (2021) ASASSN-18aan: An eclipsing SU UMa-type cataclysmic variable with a 3.6-hr orbital period and a late G-type secondary star. *PASJ* **73**, 1209
- Warner, B. (1995) *Cataclysmic Variable Stars* (Cambridge: Cambridge University Press)
- Watson, C. L., Henden, A. A., & Price, A. (2006) The International Variable Star Index (VSX). *Society for Astronom. Sciences Ann. Symp.* **25**, 47
- Zemko, P., Kato, T., & Shugarov, S. Y. (2013) Detection of change in supercycles in ER Ursae Majoris. *PASJ* **65**, 54